



A WAVEWATCH III® Model Approach to Investigating Ocean Wave Source Terms for West Africa: Input-Dissipation Source Terms

Bennet Atsu Kwame Foli^{1,2} · Joseph K. Ansong³ · Kwasi Appeaning Addo^{1,4} · George Wiafe^{1,2}

Received: 15 June 2021 / Revised: 2 December 2021 / Accepted: 10 December 2021 / Published online: 21 January 2022
© The Author(s), under exclusive licence to Springer Nature Switzerland AG 2021

Abstract

Input and dissipation source terms contribute significantly to the projection of ocean wave properties in numerical wave models. They form an integral part of the wave energy balance equation. This study investigates the appropriate input-dissipation source terms (S_{in-ds}) that best estimate the significant wave heights and wave directions in the entire West Africa region (latitudes 10° S–30° N; longitudes 35° W–15° E) and two sub-divisions (north-western or Canary Current sub-region: latitudes 10° N–25° N; longitudes 30° W–10° W, and south-eastern or Gulf of Guinea sub-region: latitudes 2° S–8° N; longitudes 10° W–10° E) using the WAVEWATCH III® (WW3) numerical ocean wave model version 5.16. Five S_{in-ds} (WAM Cycle 3, ST1; WAM Cycle 4 and variants, ST3; Tolman & Chalikov (1996), ST2; Ardhuin et al. (2010), ST4; and Zieger et al. (2015) ST6) and two additional variants (ST2STAB and ST4STAB) implemented in the WW3 model were investigated and outputs compared with field measured data from four stations in the region. For simulations of the sub-grids, ST2STAB best estimates significant wave heights for both the combined stations of the south-eastern grid and the north-western grid, whereas ST6 and ST2STAB best estimate wave directions for the respective sub-grids. For simulations of the entire West Africa grid, the S_{in-ds} that best estimate the significant wave heights are ST3, ST2STAB, ST2STAB and ST4/ST4STAB, while ST6, ST4/ST4STAB, ST2STAB and ST1 best estimate wave directions for the four respective stations. A combination of all the stations for the entire West Africa region revealed that ST2STAB best estimates significant wave heights indicated by lowest Hanna & Heinold (1985). American Petroleum Institute.) performance index (HH) and normalized bias index (NBI) values of 0.34 and –23.09% respectively. Wave directions on the other hand are best estimated by ST6 with the least NBI value and mean bias of –1.23% and –1.68±21.48°, respectively, for the entire region. ST2STAB and ST6 are thus identified to be suitable for wave height and wave direction modelling respectively for the entire West Africa region. A major conclusion of this study is that different S_{in-ds} best estimates the wave heights and directions in the West Africa region. However, ST2STAB would be the appropriate source terms to be used in projecting both wave height and direction since very little differences exist among the various source terms in projecting wave directions.

Keywords Ocean wave modelling · Input-dissipation source terms · Significant wave heights · Gulf of Guinea · WAVEWATCH III · West Africa

✉ Bennet Atsu Kwame Foli
bentsufo@yahoo.co.uk; bafoli@ug.edu.gh

¹ Department of Marine and Fisheries Sciences, College of Basic and Applied Sciences, University of Ghana, P.O. Box LG99, Legon, Ghana

² Global Monitoring for Environment and Security and Africa, College of Basic and Applied Sciences, University of Ghana, c/o P.O. Box LG99, Legon, Ghana

³ Department of Mathematics, University of Ghana, Legon, Ghana

⁴ Institute of Environment and Sanitation Studies, University of Ghana, Legon, Ghana

1 Introduction

In West Africa, scanty information on ocean wave characteristics exist. Limited research has been carried out on the parameterization of ocean wave properties with the aim of localizing global models to suit the region. In addition, there are no known regional model formulations with specific derived source terms purposely designed to study and model the surface wave characteristics in the West Africa region. Some studies have however been carried out in the region that include the description of different surface wave regimes based on global hindcast data (Olagnon et al, 2004;

Semedo, 2018) and the application of wave model output from global hindcast on the influence of beach response (Ondoa et al., 2017). The most extensive study on ocean waves in the West Africa sub-region until date has been the West African Swell Project (WASP), conducted between 1995 and 2002 to analyse and compare the available data on swells off West Africa (Olagnon et al., 2004). That study made use of a series of in situ measurements from buoys deployed in the region, hindcast data from the West Africa Normals and Extremes (WANE) project (obtained from Oceanweather), which is a follow-up of the West Africa Extreme (WAX) project, as well as the National Oceanic and Atmospheric Administration (NOAA) WAVEWATCH III model output from a global grid. Similarly, studies on ocean swell variability along the Gulf of Guinea by Toualy et al. (2015) made use of remotely sensed satellite data and model data from NOAA (WAVEWATCH III) over a relatively short period (4.5 years) to investigate the sources of swells in the region. Earlier studies by Cardone et al. (1995) also investigated extreme wave climate off the West African coast, known as the West African eXtreme Joint Industry Project (WAX JIP) using hindcast data generated with global wave parameterization schemes. In all these studies, model data used was generated on a global system using model parameterization source terms that suited wave propagation on a global scale. The use of outputs from global model formulations for regional as well as local purposes however results in systematic errors in wave properties (e.g. wave height and direction), which affect decision-making based on such model outputs.

This study is therefore aimed at providing representative wave forecasting schemes for the West Africa region. The specific objective is to investigate the ocean wave input and dissipation source terms that are appropriate for generation of accurate hindcast and forecast wave properties for the region using the WAVEWATCH III wave model. Several studies have investigated the performance of different input-dissipation source terms in different parts of the globe under different ocean conditions (Kalourazi et al., 2020; Lee, 2015; Liu et al., 2017; Montoya et al., 2013; Sheng et al., 2019; Stopa et al., 2016; Umesh & Behera, 2020; Wang et al., 2017). These studies underscore the importance of investigating the best-performing input-dissipation source terms for a particular region.

1.1 Model Description (the WAVEWATCH III Model v5.16)

The WW3 model is an enhanced third-generation wave model that has the capacity for wave hindcasting, nowcasting and short-term forecasting (Wang et al., 2017). It was developed by NOAA/National Centers for Environmental Prediction (NCEP) and became operational in March 2000

as a replacement of the Wave Action Model (WAM) (Tolman et al., 2002; Tolman & Chalikov, 1996). WW3 model replaced WAM as a result of inability of the latter to support further improvements when computer architecture was enhanced (Tolman et al., 2002). The main differences between WAM and WW3 include the use of full spectral action density equation by WW3 as well as the employment of new physics parameterizations for source terms, enabling the model to take into account large-scale wave-current interactions and efficient and more accurate numerical integration (National Weather Service, 2009; Tolman et al., 2002). WW3 also includes options for shallow-water physics and allows for new and additional physical and numerical scheme to be easily developed, as it has evolved from being a model into a modelling framework (National Weather Service, 2009).

1.2 Model Implementation

Third-generation wave models such as WW3 predict wave properties using the energy spectrum. The prediction of the energy spectrum for ocean waves stems from the complexity of wave generation and propagation of irregular wind waves. The sum of the sea state at any particular time is a result of sinusoidal waves of different wavelengths that propagate in different directions being randomly superpositioned (Tolman et al., 2002). The wave energy spectrum, represented as $F(f, \theta)$, describes the distribution of wave frequency f and propagation direction θ . The WW3 model solves for wave properties using the wave action density or wavenumber-direction spectrum N as $F(k, \theta)$ (Wang et al., 2017), where k is the wavenumber. The wavenumber-direction spectrum exhibits characteristics of invariance with respect to the physics of wave growth and decay for varying depths of water bodies (WAVEWATCH III Development Group, 2016).

The wave action density spectrum N is related to the energy density spectrum F as:

$$N = F/\theta \quad (1)$$

The wave action density equation is given as:

$$\frac{dN(k, \theta; x, t)}{dt} = \frac{S_{tot}(k, \theta; x, t)}{\sigma} \quad (2)$$

where σ is the intrinsic wave frequency and x and t are the variables of space and time, respectively.

In Equation 2, d/dt is a representation of the total derivative, whereas S_{tot} is the net effect of sources and sinks for the energy spectrum F (WAVEWATCH III Development Group, 2016). The intrinsic frequency σ relates to the wavenumber through the wave dispersion equation:

$$\sigma^2 = gk \tanh kd \quad (3)$$

where g is gravitational acceleration and d is the mean water depth.

Equation 2 assumes that the space and time scales of individual waves are much smaller compared to the corresponding changes in the spectrum as well as the mean depth and currents (Tolman et al., 2002). Equation 3 assumes a large-scale bathymetry where depths and currents vary slowly, and therefore wave diffraction can be ignored. In the WW3 package, the energy (variance) is conserved where there are no currents. However, in cases where currents exist, the energy is no longer conserved due to the contribution of currents to the mean momentum transfer of waves as indicated by Longuet-Higgins and Stewart (1961, 1962) and thus makes the wave action density spectrum a preferred choice in the WW3 model.

The energy balance equation relating the action density spectrum and incorporating wave source terms is indicated as (Liu et al., 2019; WAVEWATCH III Development Group, 2016; Zieger et al., 2015):

$$\frac{DF}{Dt} = S_{tot} = S_{in} + S_{nl} + S_{ds} + S_{ln} + S_{bot} + \dots + S_{xx} \quad (4)$$

The left side of Equation 4 describes the variance in the local spectrum as a result of individual wave energy spectra being propagated by the group velocity. The right side (S_{tot}) represents a cumulative effect of sources and sinks of wave energy. The components of these cumulative sources and sinks may comprise of wind input (S_{in}), energy dissipation as a result of wave breaking (S_{ds}) and bottom friction (S_{bot}), non-linear transfer of energy between spectral wave components (S_{nl}), linear propagation (S_{ln}) and others. The cumulative source term (S_{tot}) in deep water mainly comprise of the wind input term (S_{in}), the non-linear wave-wave interaction term (S_{nl}) and the dissipation term (S_{ds}), and the dispersion relation in Eq. 3 reduces to $\sigma^2 = gk$ (Liu et al., 2019; Swain et al., 2018). In WW3, additional processes are included when considering shallow water regimes. These include wave bottom interaction (S_{bot}), depth-induced breaking (S_{db}), wave-wave triad interaction (S_{tr}) and scattering of waves by topographic features (S_{sc}), as well as a user defined experimental source term (S_{xx}) (Umesh et al., 2018; WAVEWATCH III Development Group, 2016). This study focuses on the investigation of the wind input (S_{in}) and wave dissipation (S_{ds}) source terms, which are implemented in WW3 as combined source terms (S_{in_ds}). These are considered as part of the primary components of the energy balance equation (Tolman et al., 2002). The wave energy balance equation (Eq.4) is solved by WW3 consecutively for spatial propagation, intraspectral propagation and source terms, using a fractional step method (Umesh et al., 2018).

Wave properties such as the significant wave height (H_s) can then be estimated from the energy balance equation

and the spectrum using Eq. 5. The significant wave is derived from the energy spectrum by estimating four times the square root of the spectral moment of zero order of the wave spectrum (Kuznetsova et al., 2016; Tolman et al., 2002; Tolman & Chalikov, 1996).

$$H_s = 4 \left[\iint F(f, \theta) df d\theta \right]^{1/2} \quad (5)$$

1.3 Input and Dissipation Source Terms

WW3 mainly considers the wind input, the non-linear interaction, the bottom friction and the whitecapping dissipation source terms in resolving the wave energy balance equation (Tolman et al., 2002). It also applies several parameterisations for different processes which can be activated individually as represented by Eq.4 (Zieger et al., 2015). Here we focus on the variations of input-dissipation source terms implemented in version 5.16 of the WW3 package.

The growth of wind induced waves is generally attributed to the input energy from winds. Input energy by winds mainly contributes to the positive component of wave parameterization schemes. On the other hand, dissipation of wave energy contributes to the negative component of the wave parameterisation source term and is attributed to wave-breaking and swell attenuation (Zieger et al., 2015).

There are several options for the parameterization of the input-dissipation source term packages in WW3 version 5.16 (WAVEWATCH III Development Group, 2016). The input-dissipation parameterisation packages considered in this study are enumerated below with corresponding references for detail consultations.

- (i) WAM Cycle 3 (WAM3 or ST1) package (Komem et al., 1984; Snyder et al., 1981; Wang et al., 2017)
- (ii) Tolman & Chalikov (1996) package (TC96/TC96stab or ST2/ST2STAB) (Chalikov, 1995; Chalikov & Belovich, 1993; Tolman, 2002; Tolman & Chalikov, 1996; WAVEWATCH III Development Group, 2016)
- (iii) WAM4 and variants (WAM4+ or ST3) package (Bidlot et al., 2007; Günther et al., 1992; Janssen, 1989, 1991; Wang et al., 2017; WAVEWATCH III Development Group, 2016)
- (iv) Ardhuin et al. (2010) package (AR10/AR10stab or ST4 / ST4STAB) (Ardhuin et al., 2010; Bidlot et al., 2007; WAVEWATCH III Development Group, 2016)
- (v) Zieger et al. (2015) source term (BYDRZ or ST6) (Liu et al., 2019; WAVEWATCH III Development Group, 2016; Zieger et al., 2015)

2 Data and Methods

2.1 Study Location

This study covers the entire marine environment of the West Africa region (latitudes 10° S–30° N; longitudes 35° W–15° E) and includes the Gulf of Guinea as well as Canary Current sub-regions. These areas are important fishing grounds and shipping routes that contribute immensely to the economies of coastal West African countries as well as the World at large. The investigation of source terms was carried out for the entire region of West Africa as well as two sub-regions, which comprise the north-western section of West Africa (Canary Current region: latitudes 10° N–25° N; longitudes 30° W–10° W), and the south-eastern section (Gulf of Guinea region: latitudes 2° S–8° N; longitudes 10° W–10° E). Fig. 1 provides the map of the entire study area and the sub-grids.

2.2 Data

2.2.1 Wind Input Data

Ocean surface wind data was downloaded from the NOAA National Operational Model Archive and Distribution System (NOMADS) server and used as input data for forcing the wave model. This data is produced by NCEP and comprise of 10-m level surface zonal and meridional wind velocities. The data used is part of an operationally prepared forecast

using global Advanced Weather Interactive Processing System (AWIPS) grid at NCEP (Rutledge et al., 2006). The data is produced with a 0.5-degree latitude-longitude grid spatial resolution at a 6-h temporal resolution as part of a “Global-Multi-Grid Wave Model (Static Grids)”.

2.2.2 Observational Data

In situ wave data in the West Africa region is scanty. Observational data was obtained from three moored buoys and an Acoustic Doppler Current Profiler (ADCP). These were deployed at different periods and do not necessarily coincide with respect to time. These datasets are independent and thus very much suit the purpose of comparison with simulated data for objective accuracy assessments. Wave parameters obtained from these field measurements for the purpose of this study are significant wave height (H_s) and wave direction. The moored buoys were deployed in Cotonou in Benin (station 1, Stn1), Takoradi in Ghana (station 3, Stn3) and Mindelo in Cabo Verde (station 4, Stn4). The ADCP was deployed in Ada, also in Ghana (station 2, Stn2) as depicted in Fig. 1. These instruments measured data over short periods. In Ghana, the Datawell directional wave rider buoy DWR-MkIII was deployed by the Department of Marine and Fisheries Sciences of the University of Ghana at the western coast. The ADCP was also deployed at the eastern coast of Ghana by the International Marine and Dredging Consultants (IMDC) from Antwerp, Belgium. In Benin, an Alize Multi-parameter Oceanographic buoy was deployed by the Institut de Recherches Halieutiques et Océanologiques du

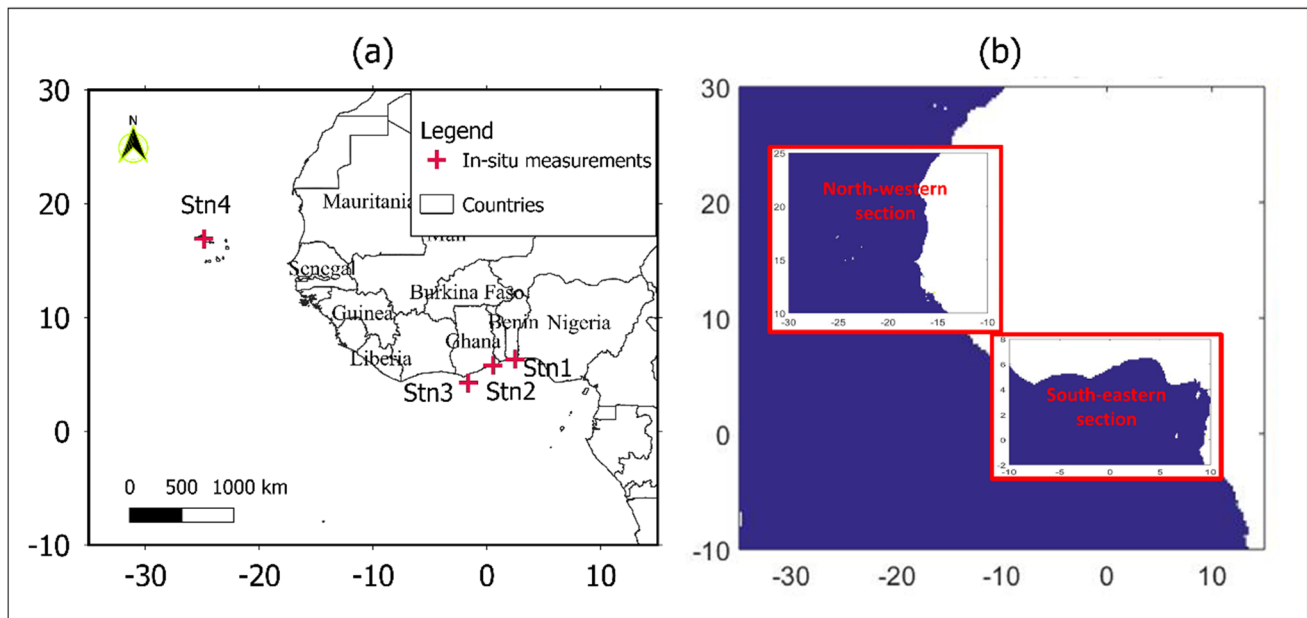


Fig. 1 Map of the entire study area indicating **a** main domain grid with stations of in situ measuring equipment (Stn1, Stn2, Stn3, Stn4) and **b** sub-domain grids for wave model simulations

Bénin (IRHOB) under the Système d'Alerte Précoce (SAP-Bénin) project, to obtain coastal wave parameters. In Cabo Verde, a TRIAXIS Next Wave II directional wave buoy was deployed by the Instituto Nacional de Desenvolvimento das Pescas (INDP) in collaboration with the University of Ghana under the European Union (EU) sponsored Monitoring for Environment and Security in Africa (MESA) project. Details of in situ measurements with locations, depth and equipment type are presented in Table 1. All in situ data were quality controlled, such as removal of extreme values that were recorded during deployment and retrieval of equipment.

In addition to in situ observations, satellite data on significant wave heights for the study periods, with spatial resolution of 1 degree, was obtained from the Archiving, Validation and Interpretation of Satellite Oceanographic data (AVISO) web portal operated by le site du Centre national d'études spatiales (CNES) in France. Also, gridded satellite wind data from L'Institut Français de Recherche pour l'Exploitation de la Mer (IFREMER) is validated with in situ wind measurements obtained from the Prediction and Research Moored Array in the Tropical Atlantic (PIRATA) program and compared with the model wind data used for the wave simulations.

2.3 Wave Model Setup

2.3.1 Generation of Spatial Grids

The study utilized the WAVEWATCH III® version 5.16 for investigating the input-dissipation source terms for ocean wave modelling. Model domain grids were generated with the GRIDGEN code of Chawla and Tolman (2007) that

accompanied the WW3 model. The GRIDGEN code is a MATLAB® grid generation software for automated generation of model domain grids to user specifications. Three spatial grids were used for investigating input-dissipation source terms. The main grid covered the entire West Africa region with a resolution of 0.25 degrees and two additional sub-grids which cover the north-western and south-eastern sections of the main grid, both with higher resolution of 0.125 degrees. All domains utilized regular rectilinear grids with bathymetry data extracted from ETOPO2, provided by the National Geophysical Data Center of NOAA.

2.3.2 Wave Model Parameterization Schemes

Five different input-dissipation source term configurations (S_{in-ds}) of the WW3 model were implemented in order to assess the performance of wind input and wave dissipation source terms collectively. All results for the different input-dissipation source terms were obtained with the discrete interaction approximation (DIA) non-linear wave-wave interaction source term of Hasselmann et al. (1985) and the linear input propagation source term parameterization of Cavaleri and Malanotte-Rizzoli (1981). Parameterization of bottom friction employed the Joint North Sea Wave Project (JONSWAP) bottom friction formulation (Hasselmann et al., 1973) together with the depth-induced breaking parameterization of Battjes-Janssen (Battjes & Janssen, 1978). A linear wind interpolation method implemented in WW3 was applied for temporal and spatial wind interpolation. A Fetch-limited JONSWAP spectrum, i.e. spectrum calculated using local wind and direction, was used as initial condition at the open boundaries, while other boundary conditions were

Table 1 Location of field wave measurements where in situ data was obtained with collocated data period for model data comparison

Station ID	Station name/location	Longitude	Latitude	Equipment type	Data source (institution)	Estimated depth of station (m)	Collocated data period/model ran periods (yyyymmdd)
Stn1	Cotonou, Benin	2.470267	6.308133	Alize Multi-parameter Oceanographic buoy	Institut de Recherches Halieutiques et Océanologiques du Bénin (IRHOB) (IRHOB), Benin	16.5	20151215–20160209
Stn2	Ada, Ghana	0.52496	5.77210	Teledyne RD ADCP	International Marine and Dredging Consultants (IMDC), Antwerp, Belgium	11.5	20100219–20100316
Stn3	Takoradi, Ghana	−1.62749	4.23164	Datawell Directional Wave buoy	Department of Marine and Fisheries Sciences, University of Ghana	170	20111012–20111121
Stn4	Mindelo, Cabo Verde	−24.8715	16.8901	Triaxys Wave buoy	GMES and Africa programme, University of Ghana	70	20160204–20160412

Table 2 Time steps and spectral discretization parameterizations used in the WW3 model setup

Parameterization scheme	Main grid	Sub-grids
Overall/global time step	Max 900 s	Max 450 s
CFL/spatial propagation time step	Max 950 s	Max 475 s
Maximum refraction (and wavenumber shift) time step	450 s	225 s
Source term integration time step	Min 15 s	Min 15 s

Table 3 Input-dissipation source term switches deployed in the WW3 model for the study

Switch ID	Summary description	Reference
ST1	WAM Cycle 3	WAM3
ST2	Tolman & Chalikov (1996)	TC96
ST2STAB	Tolman & Chalikov (1996) with wind correction factor	TC96stab
ST3	WAM Cycle 4 and variants	WAM4+
ST4	Ardhuin et al. (2010)	AR10
ST4STAB	Ardhuin et al. (2010) with wind correction factor	AR10stab
ST6	Zieger et al. (2015)	BYDRZ

based on the gridded input wind data. All other parameterization schemes and constants were maintained as for the default WW3 model setup. Time steps and spectral discretization used are presented in Table 2 for the main grid and sub-grids following the recommendation of Tolman & Chalikov (1996). Seven combinations of input-dissipation source terms presented in Table 3 were varied for this study.

With a spatial resolution of $0.25^\circ \times 0.25^\circ$, the main grid consisted of 201×161 points of which 19070 (58.9%) are sea points on a rectilinear grid. The north-western and the south-eastern sub-grids both with a resolution of $0.125^\circ \times 0.125^\circ$ consisted respectively of 161×121 points and 161×81 points with 13089 (67.2%) and 8916 (68.4%) sea points, respectively. The spectrum for the main grid as well as the sub-grids is discretized with 32 frequencies, ranging from 0.0373 to 0.7159 Hz with an increment factor of 1.1 and 36 directions with a 10-degree directional increment. The remaining details of the model settings follow the default setup, and further details can be found in the user manual and system documentation of WAVEWATCH III® version 5.16 (WAVEWATCH III Development Group, 2016).

2.4 Statistical Comparisons

Statistical parameters used for comparing the output of the various simulations to in situ measurements include estimation of mean bias ($\bar{\mu}$) with standard deviations (σ) and correlation coefficients (r). The bias is the difference between the

model results and measured data. Lower values of σ indicate better fit between model outputs and observed data. In addition to these parameters, a normalized bias index (*NBI*) and an accuracy performance index known as the symmetrically normalized root mean square error (HH) proposed by Hanna and Heinold (1985) as cited in Mentaschi et al. (2013) were computed. The Hanna and Heinold (1985) index has been argued by Mentaschi et al. (2013) to best determine the accuracy of models because the RMSE, normalized RMSE (NRMSE) and scatter index (SI) are not always reliable in assessing the accuracy of numerical models. In their investigations, Mentaschi et al. (2013) found that small values of RMSE, NRMSE and SI are not always able to differentiate the best performance of a numerical simulation. Lower values of HH and NBI values close to zero indicate best fit between model and observed data. Scatter plots were also conducted for comparison. The statistical parameters used are defined as follows:

$$\bar{\mu} = \frac{1}{N} \sum_{i=1}^N (S_i - O_i) \quad (6)$$

$$\sigma = \sqrt{\frac{\sum (\mu - \bar{\mu})^2}{N}} \quad (7)$$

$$r = \frac{(N \sum_{i=1}^N S_i O_i - \sum_{i=1}^N S_i \sum_{i=1}^N O_i)}{\sqrt{[N \sum_{i=1}^N S_i^2 - (\sum_{i=1}^N S_i)^2][N \sum_{i=1}^N O_i^2 - (\sum_{i=1}^N O_i)^2]}} \quad (8)$$

$$NBI = \frac{(\bar{S} - \bar{O})}{\bar{O}} \quad (9)$$

$$HH = \sqrt{\frac{\sum_{i=1}^N (S_i - O_i)^2}{\sum_{i=1}^N S_i O_i}} \quad (10)$$

where S_i and O_i are the i th values for simulated and observed data, respectively, N is number of observations for the analysis, \bar{S} and \bar{O} are average simulation and observation values, respectively, and μ represents individual bias or residual values.

3 Results and Discussions

Results from the WW3 simulations with varying input-dissipation source terms (S_{in-ds}) are presented. The study utilized five main S_{in-ds} source terms, and in two of them, wind correction factor was applied. Thus, a total of seven

S_{in-ds} were used in investigating the behaviour of ocean wave parameters in the West Africa region. The simulation outputs are here compared with in situ wave data obtained from four different wave measurement locations in the region (see Fig. 1 and Table 1). Results are presented for simulations conducted for the entire study area as well as for two subdivisions, i.e. the north-western and south-eastern grids (see Fig. 1).

Significant wave heights from in situ measurements taken at the various stations in the West Africa region are compared with satellite data in Fig. 2. The satellite measurements at stations 1, 3 and 4 agree quite well with in situ data. Deviations are largest at station 2, possibly as a result of close proximity to the coast, thus contaminating the satellite measurements which have a coarse spatial resolution.

NCEP wind data used for simulating the wave model was compared with satellite wind observations (Fig. 3). Validation of the satellite wind observations with in situ measurements from the PIRATA programme (combined data for two locations each in the south-eastern and north-western sections—see Foli et al. (2021)) shows very good agreements with little variations at certain points (Fig. 4). The comparison of NCEP model winds with satellite observations shows better agreements at the north-western (NW) section compared to the south-eastern (SE) section of the study area. This indicates that accuracy of the NCEP model winds is better in the NW section compared than the SE section of the West Africa region. Investigations by Foli et al. (2021) indicated better estimation of meridional winds in the NW

than the SE section by NCEP winds. This variation in NCEP wind accuracies in the region will also have an impact on wave projections for the region.

Simulation outputs show that wave heights and directions from most of the input-dissipation source terms have some level of agreement with in situ data at the various stations. The simulations conducted for seven different combinations of input-dissipation source terms are represented by ST1, ST2, ST2STAB, ST3, ST4, ST4STAB and ST6 as defined in Table 3. The results for ST4 and ST4STAB were noted to be the same for all grids and so are represented with only ST4.

3.1 West Africa Grid

A time-series plot of significant wave heights (H_s) and wave height residuals for the West Africa grid (Figs. 5 and 6) shows that outputs for source terms at station 4 (Stn4) exhibit the closest agreement with measured data. This is closely followed by station 2 (Stn2). A scatter plot of measured H_s against model H_s (Fig. 7) clearly indicates station 1 (Stn1) as the location where there is least performance of the source terms against measured data. This situation is similar for the wave direction as well (Figs. 7 and 8). This is a clear indication of the variable performances of the input-dissipation source terms at the various locations in the region. A comparison of the in situ measurement with satellite observations presented in Fig. 2 for station 1, which shows good agreement, vindicates the in situ measurements are the cause of the large deviations. The abysmal performance

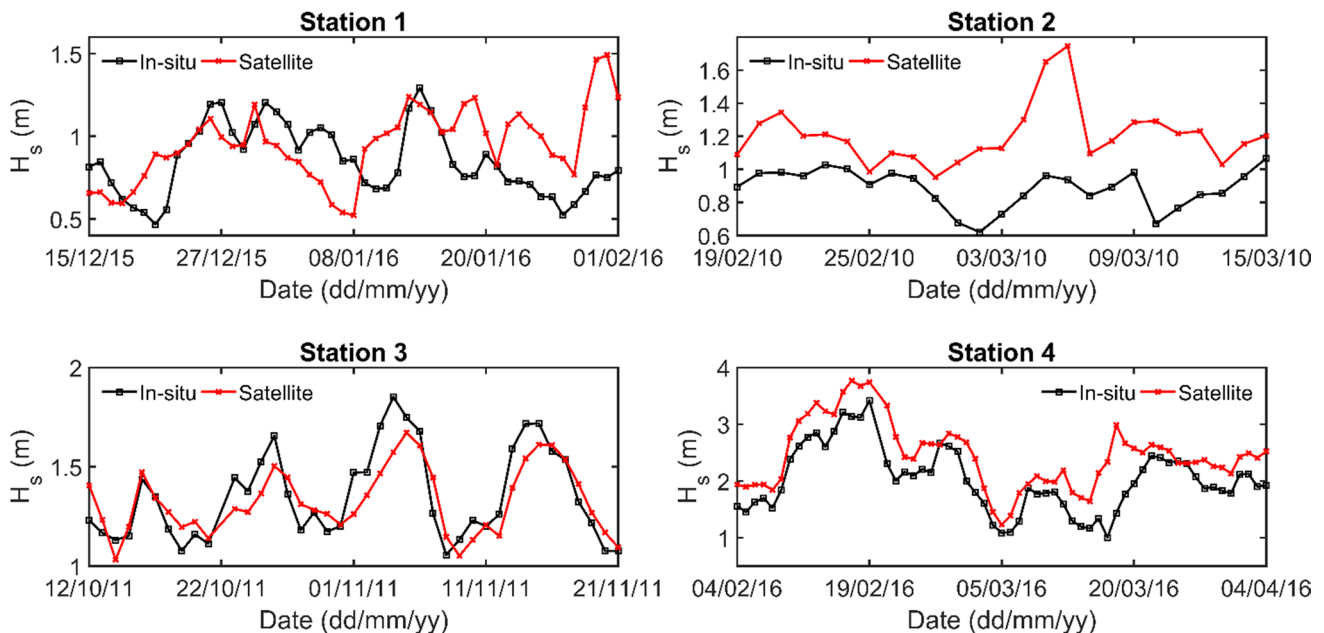
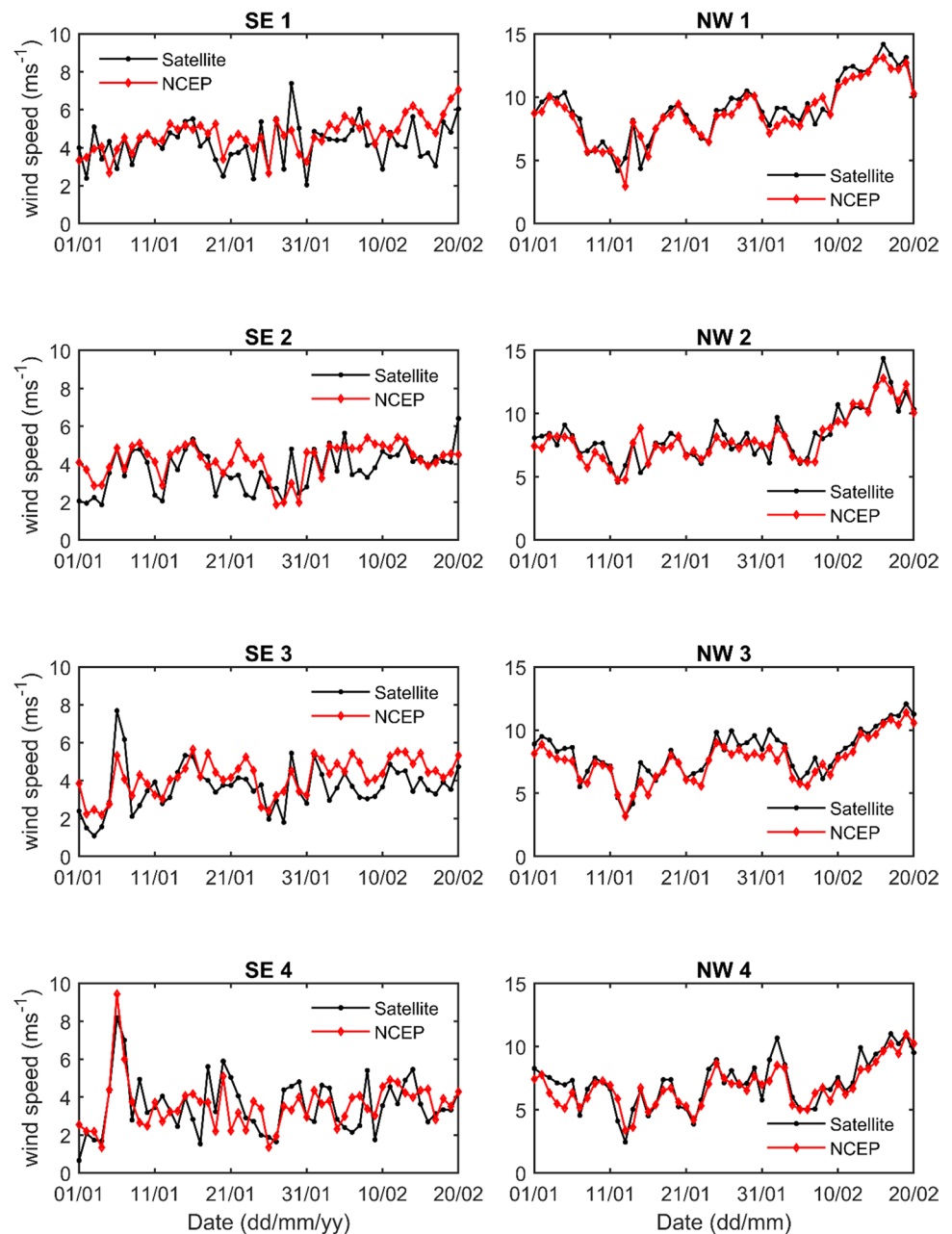


Fig. 2 Comparison of in situ significant wave height (H_s) measurements with satellite data from AVISO at the various stations. Black solid lines represent in situ measurements, while red solid lines represent satellite measurements

Fig. 3 Model wind data from NCEP used in the wave simulations compared with satellite measurements from four different locations for the south-eastern (SE) and north-western (NW) sections of the study area. Black solid lines represent satellite measurements, while red solid lines represent NCEP model data



of the model output at Stn1 could be attributed to the fact that this is a coastal environment and likely experiences the effect of strong local currents (Chen, 2018; Zhang et al., 2021) as well as inaccuracies in the bathymetry (Arbic et al., 2019; Chen et al., 2018; Herterich & Dias, 2019) which can affect wave projections. The accuracy of the wind forcing at this location can also not be overlooked as effects of orography and coastal geometry could be stronger, leading to large errors in the wind input (Cavaleri et al., 1991; Desbiolles et al., 2014). The high degree of agreement of simulation outputs with in situ data observed at Stn4 may be attributed to a much accurate wind input at this location. Stn4 is located close to an island (Cabo Verde), in the middle of the

Eastern Tropical Atlantic Ocean. Therefore, the station may have less influence of contamination due to orography and coastal geometry from the large continental landmass with respect to the winds in contrast to Stn1 and Stn3.

The performance of source terms at Stn1 indicate that they all exhibit poor correlations of model wave height and direction against measured data (Tables 4 and 5). The poor performance is also reflected in other performance indices such as the HH and NBI. Nonetheless, the results seem to suggest that ST3 provides the best representation for this location with respect to estimation of significant wave height. This is observed from the values of HH index and NBI recorded in Table 4. The wave direction estimations

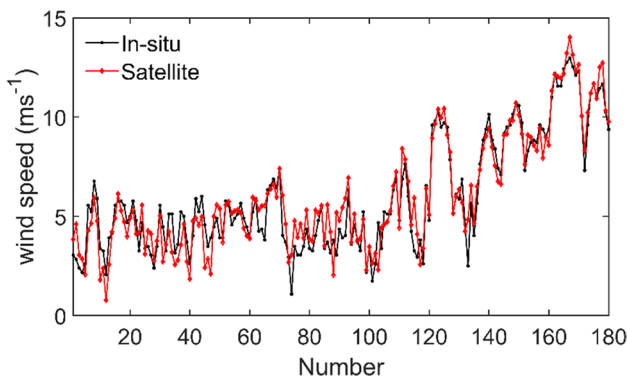


Fig. 4 Satellite wind data validated with PIRATA in situ measured data. Black solid lines represent in situ measurements, while red solid lines represent satellite measurements

at Stn1 also follows similar trajectory (Figs. 8, 9 and 10). However, lower values of NBI are recorded for wave directions (Table 5) compared to those of significant wave height. Although correlations are positive, they are almost close to zero. Results for Stn1 also suggest ST6 as the best input-dissipation source term for this location with respect to wave direction estimation. This is followed closely by ST3. Figure 11 provides a summary of the performance by each source term in a plot of HH index against the NBI. In this plot, the best source term is shown to have the least HH and with NBI closest to zero.

At Stn2, ST2STAB outperforms all the input-dissipation source terms with respect to wave heights. This is seen in Figs. 5, 6 and 7 and also demonstrated in Fig. 11. ST2STAB

recorded the least HH, NBI and a relatively high correlation coefficient with values of 0.198, -15.91 and 0.78% , respectively. It also records a mean significant wave height bias with standard deviation of -0.14 ± 0.08 m (see Table 3). The same wave height bias standard deviation was recorded for all source terms at Stn2. ST4 closely followed ST2STAB in performance with mean bias of -0.16 m, with correlation coefficient and HH and NBI values of 0.8, 0.218 and -17.79% , respectively. Wave direction at Stn2 is best estimated by ST4 with HH and NBI of 0.061 and 0.89% , respectively. This is again followed closely by ST3, also with HH and NBI of 0.064 and 3.63% , respectively.

Significant wave height at Stn3 was observed to be better estimated again by ST2STAB and ST4, with ST2STAB outperforming all, followed by ST4 (Figs. 5, 6, 7 and 11). Although ST2 and ST6 recorded the least bias standard deviations for Stn3, they recorded relatively high mean biases of -0.85 m and -0.86 m, respectively (Table 4). Very low correlation coefficients are recorded by the source terms at this location although they are significant, except for ST1. Percentage underestimation of significant wave heights by the source terms as indicated by the NBI is also high and comparable to those of Stn1.

Although high values of mean bias, HH and NBI were recorded by the source terms for significant wave heights at Stn3, the opposite is true for wave directions. All source terms demonstrated high level of performance in comparison with measured data for wave directions. Correlation coefficients are comparatively higher for wave directions than for significant wave heights at this station. While significant wave heights are highly underestimated by $50.12\text{--}67.8\%$

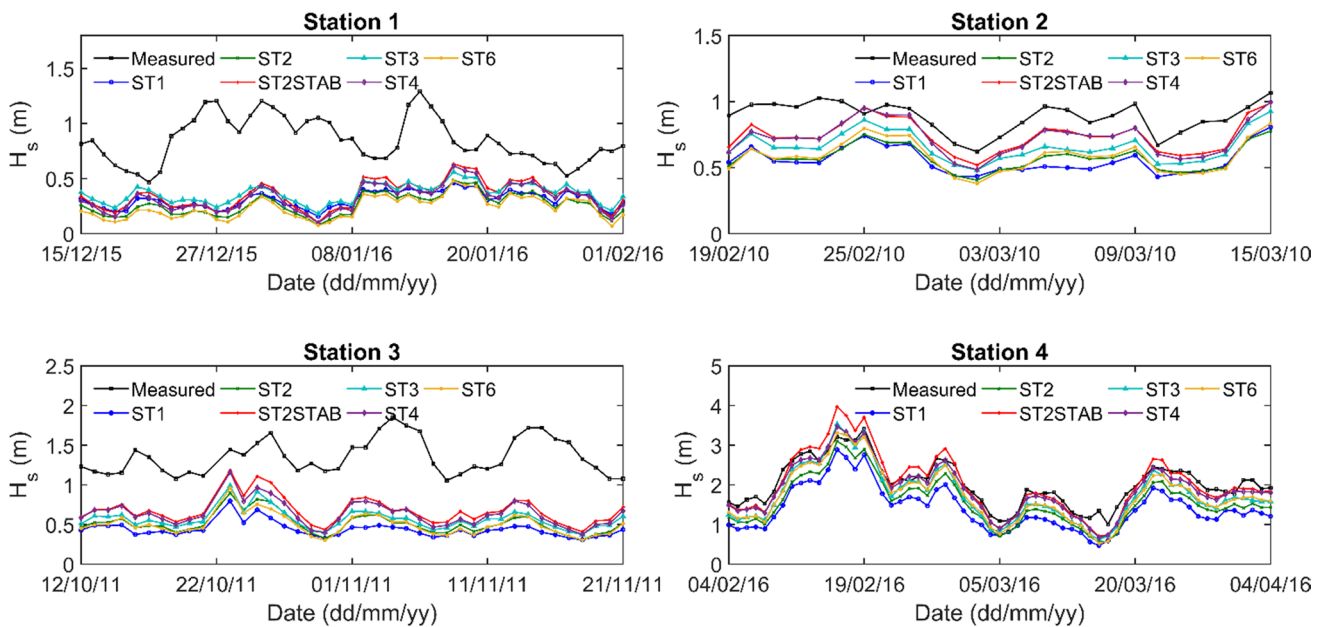


Fig. 5 Time series plot of significant wave height (H_s) outputs for the West Africa grid

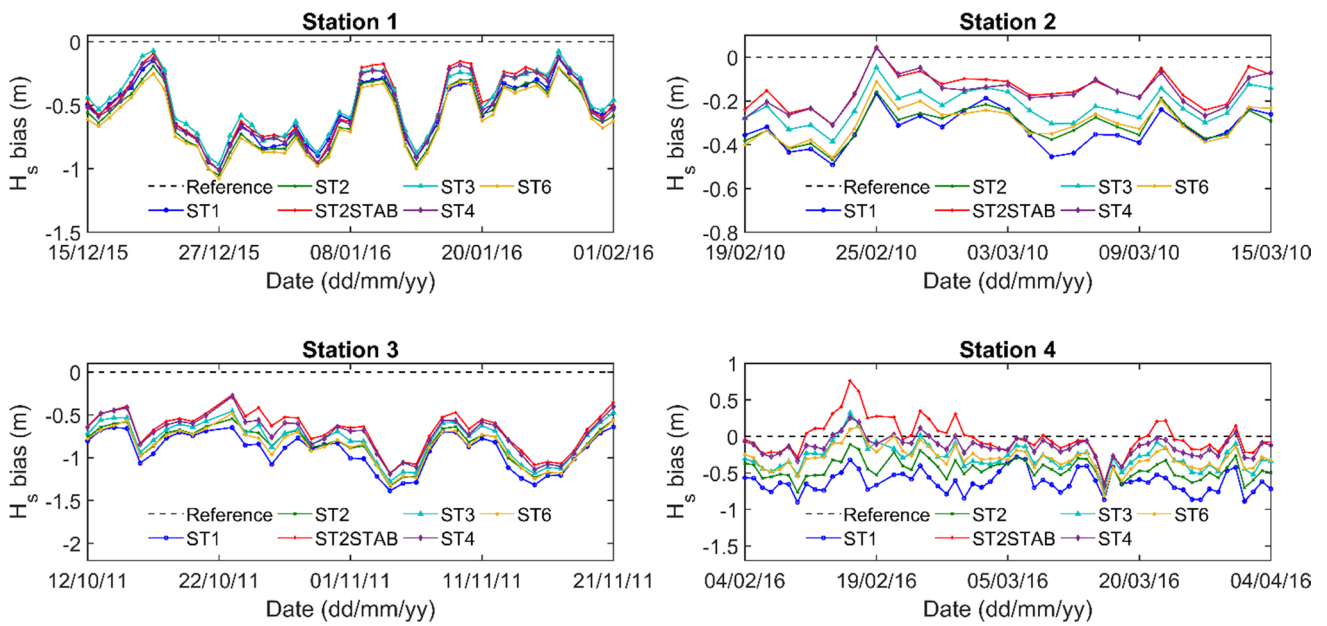
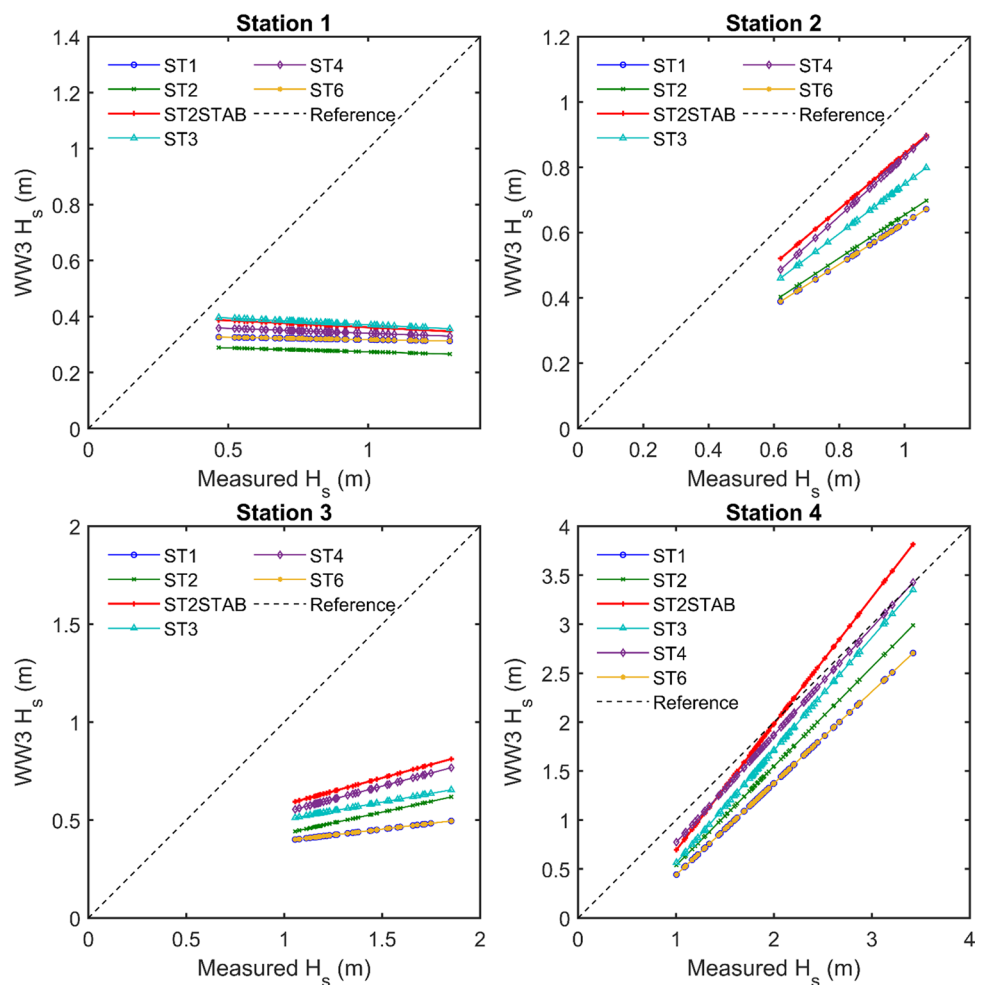


Fig. 6 Time series plot of wave height residuals/bias for the West Africa grid

Fig. 7 Scatter plot of measured significant wave heights (H_s) against model significant wave heights for the West Africa grid. Black dotted lines are references, while solid lines are the linearly fitted lines for the various model source terms



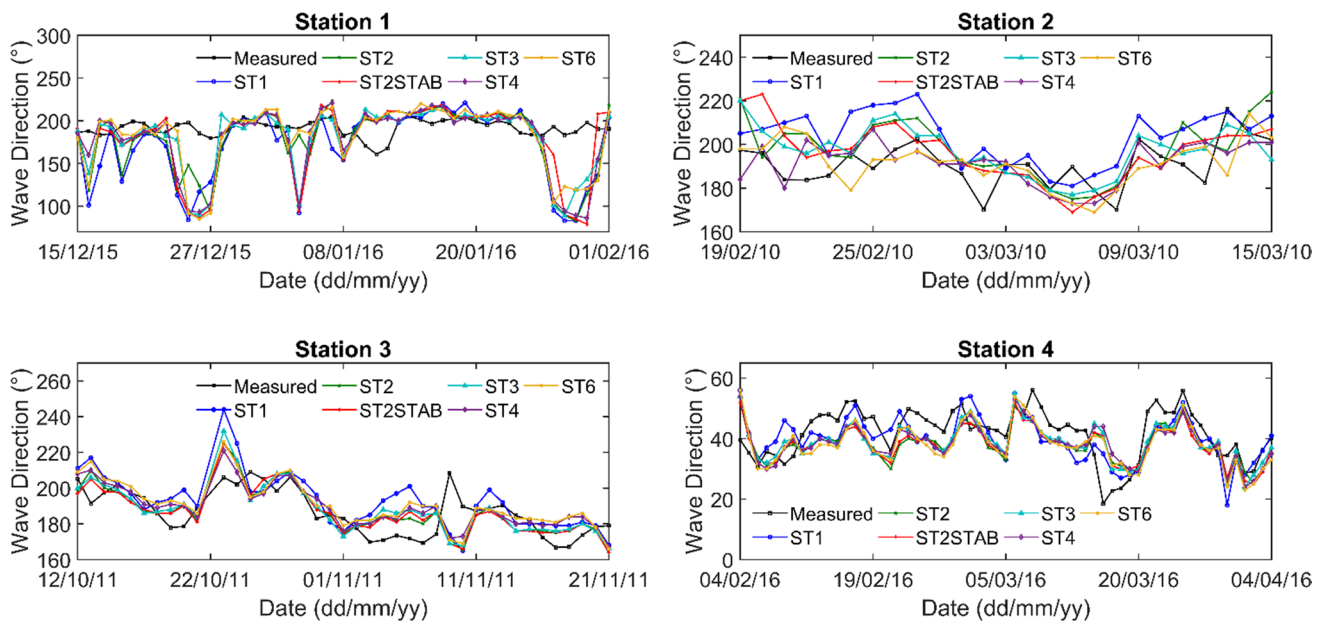


Fig. 8 Time series plot of wave direction outputs for the West Africa grid

(Table 4), wave directions on the other hand are only marginally overestimated by 0.26–3.29% (Table 5) for the source terms. ST2 and ST2STAB recorded relatively high correlation coefficients of 0.63 and 0.62, respectively, compared to the other source terms with lower correlations. The ST2 and ST2STAB source terms outperform the others with respect to the other estimated performance indices. HH indices recorded by ST2 and ST2STAB were similar. However, ST2STAB records lower mean bias as well as percentage error (NBI). The scatterplot (Fig. 10) shows how indistinctive ST2 and ST2STAB are. Figure 11 however differentiates these two source terms, indicating ST2STAB as the best-performing input dissipation source term for wave direction estimation at station 3.

All source terms performed competitively well at Stn4 with minimal variations with respect to both significant wave heights and wave directions for the entire West Africa grid. This can be seen in the scatterplots shown in Figs. 7 and 10. Mean bias for significant wave height ranged from -0.62 to -0.02 m with ST2STAB recording the least. Station 4 recorded the highest correlation coefficient values for all source terms for both wave heights and directions from among all the stations. While correlation coefficients of significant wave heights ranged from 0.97 to 0.98 (Table 4), those of wave directions were observed to be 1 for all source terms (Table 5). This indicates that the projection of wave height and direction at this location is more accurate compared to the other stations. A similar situation was noticed for reanalysis wind comparisons for the region performed by Foli et al. (2021), where modelled winds in comparison with in situ measurements recorded the best performance around

this location. This could indeed suggest that much of the differences in the modelled wave in this study can be attributed to the wind input used to force the model. This assertion is supported by the comparison of model winds with satellite data for the regions of the various stations (Fig. 3), where the model winds perform better in the north-western section (Stn4) compared to the south-eastern section (Stn1, Stn2 and Stn3). Indeed, several studies (Ponce de León et al., 2008; Schmidt et al., 2017; Tolman et al., 2002) have indicated that the accuracy of modelled waves and other numerical weather predictions depends heavily on the accuracy of the wind source or atmospheric forcing.

The best-performing input-dissipation source term for significant wave height estimations is identified for station 4 to be ST4 with HH of 0.095 and with percentage underestimation of wave heights (NBI) to be 6.75%. This is again followed closely by ST2STAB with HH of 0.107 and with percentage underestimation of 1.15%. Although ST2STAB recorded a lower mean bias and a lower NBI, ST4 recorded lower standard deviation of the mean bias in addition to a lower HH, which is an indicator of best performance. Similarly, the best-performing source term for wave direction estimations at Stn4 is identified as ST1 having HH of 0.172 and NBI of -3.68 . This is followed closely by ST3 also with HH of 0.172 but with higher NBI of -6.04% (see Fig. 11 and Table 5).

The degree of underestimation of significant wave height for the input-dissipation source terms for the entire West Africa grid ranged from 56.08 to 70.36%, 15.91 to 37.11%, 50.12 to 67.8% and 6.75 to 31.43% for stations 1 to 4, respectively, as indicated by NBI values. Similarly, the

Table 4 Summary of wave height statistics for comparisons of model simulations with in situ measurements for the entire West Africa grid

Location	Source term	Mean bias (m)	Bias standard deviation (m)	Correlation coefficient (<i>r</i>)	HH index	NBI (%)
Station 1	ST1	−0.54	0.22	−0.04	1.11	−62.78
	ST2	−0.58	0.23	−0.05	1.28	−67.66
	ST2STAB	−0.49	0.25	−0.08	0.977	−57.12
	ST3	−0.48	0.23	−0.11	0.937	−56.08
	ST4	−0.51	0.24	−0.06	1.044	−59.84
	ST6	−0.6	0.23	−0.02	1.381	−70.36
Station 2	ST1	−0.33	0.08	0.72*	0.478	−37.11
	ST2	−0.31	0.08	0.77*	0.438	−34.7
	ST2STAB	−0.14	0.08	0.78*	0.198	−15.91
	ST3	−0.22	0.08	0.78*	0.306	−25.28
	ST4	−0.16	0.08	0.8*	0.218	−17.79
	ST6	−0.3	0.08	0.77*	0.421	−33.54
Station 3	ST1	−0.92	0.22	0.29	1.221	−67.8
	ST2	−0.85	0.21	0.39*	1.043	−62.48
	ST2STAB	−0.68	0.23	0.37*	0.742	−50.12
	ST3	−0.79	0.22	0.32*	0.93	−58.25
	ST4	−0.72	0.22	0.38*	0.806	−53.15
	ST6	−0.86	0.21	0.42*	1.067	−63.38
Station 4	ST1	−0.62	0.14	0.97*	0.371	−31.43
	ST2	−0.45	0.13	0.97*	0.257	−22.76
	ST2STAB	−0.02	0.22	0.98*	0.107	−1.15
	ST3	−0.29	0.17	0.97*	0.174	−14.58
	ST4	−0.13	0.14	0.98*	0.095	−6.75
	ST6	−0.3	0.15	0.98*	0.175	−15.11
All Stations	ST1	−0.62	0.25	0.91*	0.58	−45.34
	ST2	−0.55	0.25	0.92*	0.5	−40.46
	ST2STAB	−0.32	0.34	0.93*	0.34	−23.09
	ST3	−0.44	0.28	0.92*	0.41	−32.35
	ST4	−0.37	0.3	0.92*	0.36	−27.29
	ST6	−0.51	0.29	0.92*	0.46	−37.09

*Indicates significant correlations, i.e. $p < 0.05$

degree of underestimation of wave direction for the same grid was from 4.69 to 9.03% and 3.68 to 8.72% for stations 1 and 4, respectively, while stations 2 and 3 recorded degrees of overestimations from 0.64 to 7.2% and 0.26 to 2.38%, respectively.

A combination of the extracted wave parameters for all the stations in the West Africa grid (all stations; Tables 4 and 5) compared with combined in situ measurement also yielded strong correlation coefficients with values ranging from 0.91 to 0.93 for significant wave heights and from 0.94 to 0.96 for wave directions. Percentage error estimations (NBI) for the combined stations ranged between underestimation of 23.09 to 45.34% for significant wave heights and 1.02 to 2.01% for wave directions. For the combined stations, ST2STAB recorded the best performance for the entire West Africa grid with respect to significant wave height estimations. ST2STAB recorded the least HH and NBI values of

0.34 and −23.09%, respectively. It also recorded the highest correlation coefficient (0.93), with the lowest mean bias of -0.32 ± 0.34 m. Wave directions on the other hand are best estimated for the combined locations by ST6, with the least NBI value and mean bias of -1.23% and $-1.68 \pm 21.48^\circ$, respectively. This is followed closely by ST3 also with NBI value and mean bias of -1.26% and $-1.73 \pm 22.11^\circ$, respectively. Although all the source terms recorded very close HH, ST6 and ST3 have been indicated to best estimate the wave direction with respect to all the stations combined. Fig. 11 shows the close association of ST3 and ST6 for wave direction.

3.2 Sub-grids of West Africa

The sub-grids of the West Africa region comprised the south-eastern section and the north-western section as

Table 5 Summary of wave direction statistics for comparisons of model simulations with in situ measurements for the entire West Africa grid

Location	Source term	Mean bias (°)	Bias standard deviation (°)	Correlation coefficient (<i>r</i>)	HH index	NBI (%)
Station 1	ST1	−13.43	41.63	0.06	0.236	−7.04
	ST2	−7.88	37.86	0.14	0.205	−4.13
	ST2STAB	−7.53	40.87	0.1	0.22	−3.95
	ST3	−7.04	37.19	0.07	0.2	−3.69
	ST4	−8.16	39.42	0.09	0.214	−4.28
	ST6	−4.97	35.97	0.15	0.191	−2.61
Station 2	ST1	13.73	11.76	0.48*	0.091	7.2
	ST2	7.65	12.45	0.47*	0.074	4.01
	ST2STAB	6.03	12.04	0.49*	0.068	3.17
	ST3	6.92	10.63	0.53*	0.064	3.63
	ST4	1.69	11.85	0.35	0.061	0.89
	ST6	1.23	12.61	0.3*	0.065	0.64
Station 3	ST1	6.14	14.07	0.51*	0.08	3.29
	ST2	0.86	11.22	0.63*	0.059	0.46
	ST2STAB	0.49	11.35	0.62*	0.06	0.26
	ST3	1.56	12.1	0.58*	0.064	0.84
	ST4	2.91	11.12	0.6*	0.06	1.56
	ST6	4.44	11.92	0.57*	0.066	2.38
Station 4	ST1	−1.53	7.01	1*	0.172	−3.68
	ST2	−3.27	6.34	1*	0.176	−7.84
	ST2STAB	−3.44	6.28	1*	0.177	−8.26
	ST3	−2.52	6.6	1*	0.172	−6.04
	ST4	−3.25	6.85	1*	0.187	−7.8
	ST6	−3.64	6.75	1*	0.19	−8.72
All Stations	ST1	−1.4	25.95	0.94*	0.17	−1.02
	ST2	−2.29	22.54	0.95*	0.15	−1.68
	ST2STAB	−2.55	23.91	0.95*	0.16	−1.86
	ST3	−1.73	22.11	0.96*	0.14	−1.26
	ST4	−2.76	23.17	0.95*	0.15	−2.01
	ST6	−1.68	21.48	0.96*	0.14	−1.23

*Indicates significant correlations, i.e. $p < 0.05$

depicted in Fig. 1. The south-eastern grid encompassed three in situ measurement stations, which are Stn1, Stn2 and Stn3. Figure 12 provides a time-series plot of the significant wave heights and directions, while Fig. 13 provides the time-series plot of the residual (bias) of the significant wave heights and directions of the south-eastern section. It can be observed from these figures that in general, there is better agreement of the modelled wave properties (wave heights and directions) with in situ measurement at Stn2 compared to Stn1 and Stn3 of the south-eastern grid.

At station 1, ST3 is observed to outperform other input-dissipation source terms for estimating significant wave height (Table 6), whereas ST6 best estimates the wave direction (Table 7). At station 2, however, while ST2STAB best estimates the significant wave heights, ST6 again best estimates the wave direction (Fig. 14). Again ST2STAB outperforms all other source terms in estimating the significant

wave heights at station 3, while ST2 best estimates the wave direction, closely followed by ST2STAB. A combination of all stations of the south-eastern grid also shows that ST2STAB outperforms other input-dissipation source terms in estimating significant wave heights, whereas ST6 best estimates the wave directions followed closely by ST2STAB. This is also presented in Fig. 15 with the plot of HH against NBI.

The north-western section which comprised of only station 4 shows high agreement with measured data similar to the observed data for the same station in the West Africa grid. Fig. 16 shows how close modelled wave properties are to measured data. ST2STAB recorded the highest performance for estimating both significant wave heights and wave directions at station 4 for the north-western grid (Fig. 17). It recorded the lowest mean bias, HH and NBI of -0.12 ± 0.23 m, 0.128 and -6.1% , respectively, for the significant wave

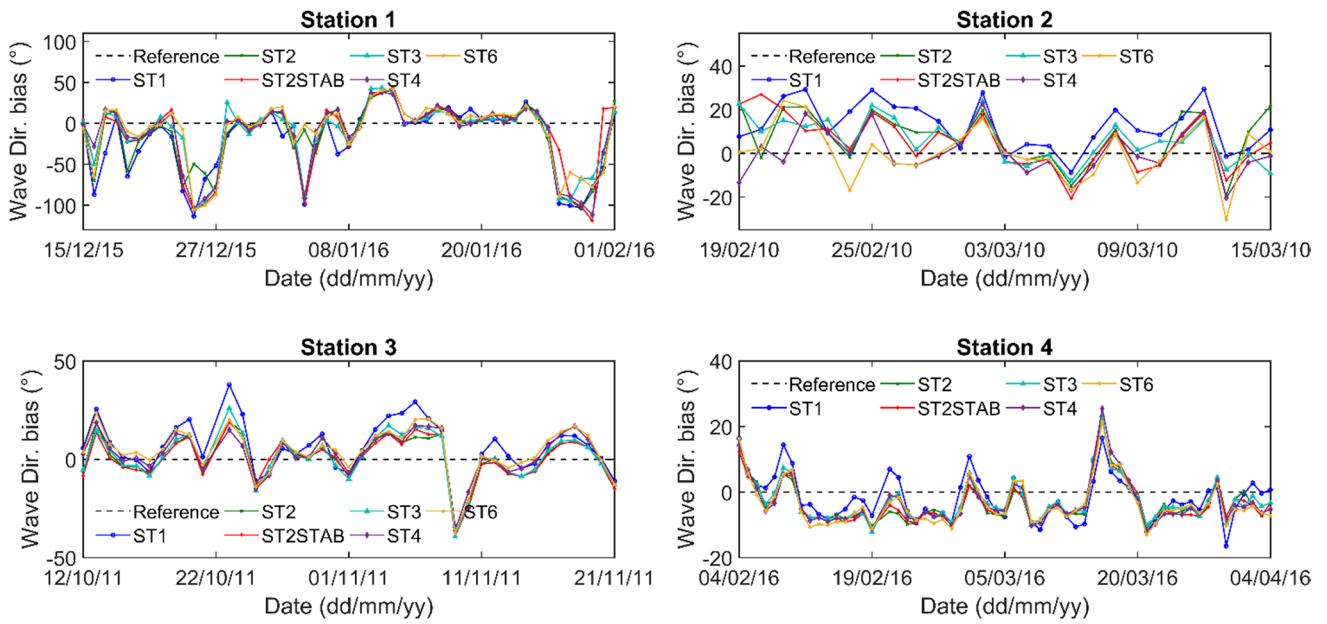


Fig. 9 Time series plot of wave direction residuals/bias for the West Africa grid

Fig. 10 Scatter plot of measured against model wave directions for the West Africa grid. Black dotted lines are references, while solid lines are the linearly fitted lines for the various model source terms

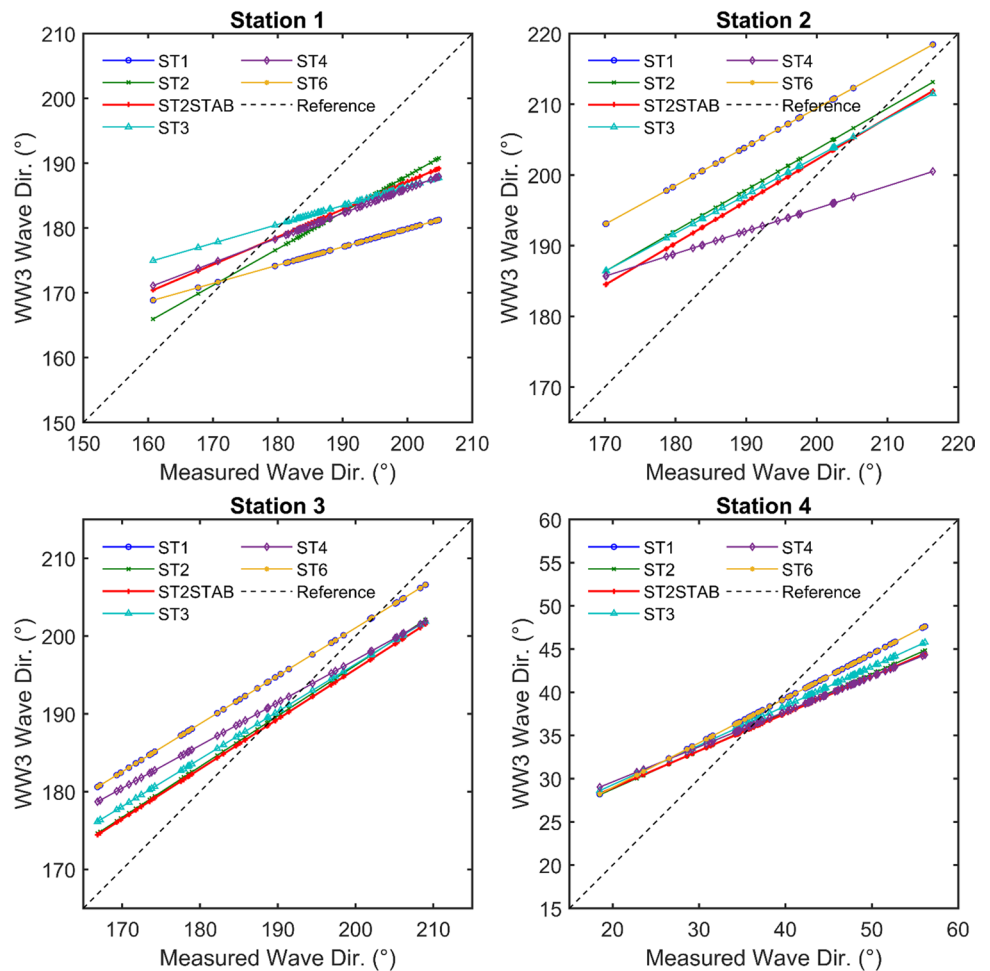


Fig. 11 Plots of HH against NBI for significant wave heights (left) and wave directions (right) for all stations of the West Africa grid

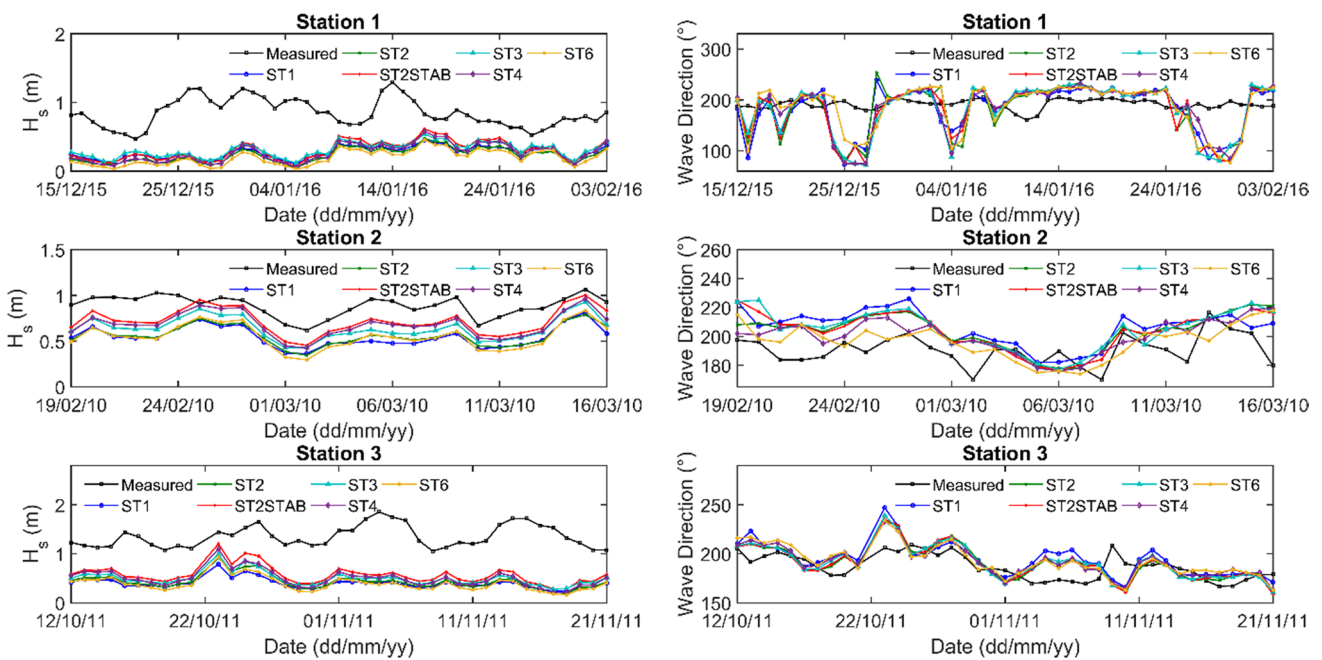
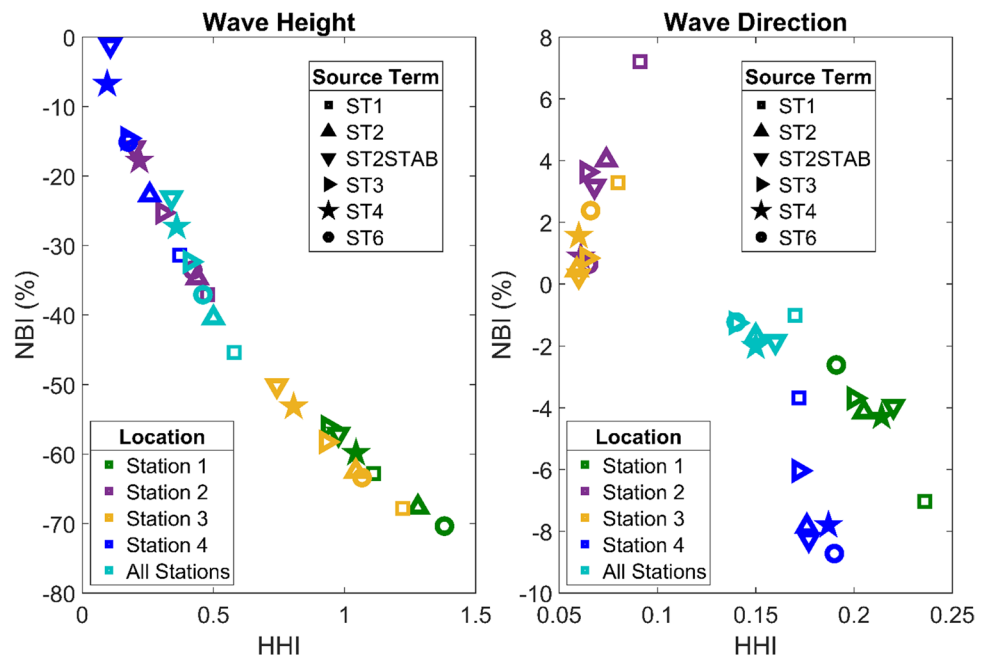


Fig. 12 Time series plot of significant wave height (left) and wave direction (right) outputs for the south-eastern grid

height estimations. Similarly, lowest mean bias, HH and NBI of 0.32 ± 6.34 m, 0.149 and 0.77% were also respectively recorded for the wave direction estimations. Besides ST2STAB, ST3 also performed relatively well for wave direction estimations for the north-western grid.

The source terms that best estimate the significant wave height and direction for the entire West Africa grid are the same for combined stations in the south-eastern grid. These are ST2STAB and ST6 for the significant wave height and

direction, respectively. Similarly, both significant wave height and direction are best estimated by only ST2STAB for the north-western grid. There is greater variability in the source terms that best estimate wave directions for specific locations or smaller regions compared to significant wave height estimations.

Generally, better performance indices are observed for simulations of the West Africa grid (Tables 4 and 5) compared to the simulations of the sub-grids with higher

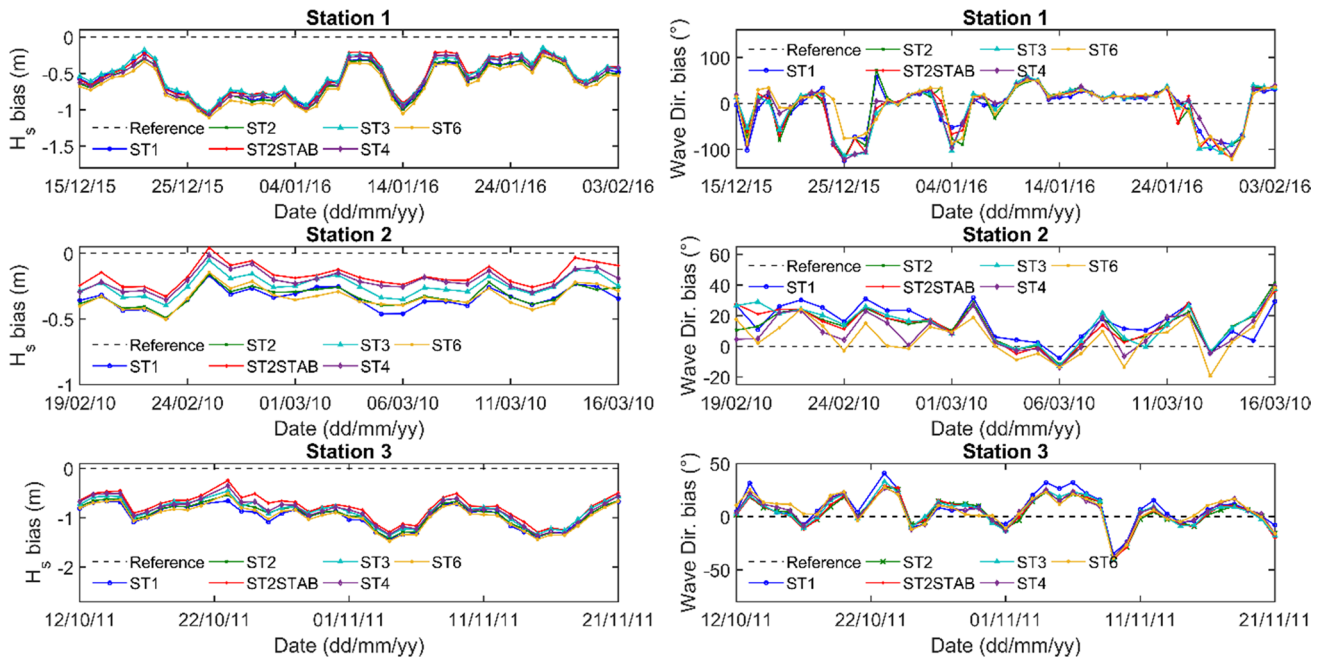


Fig. 13 Time series plot of residuals/bias of significant wave height (left) and wave direction (right) outputs for the south-eastern grid

Fig. 14 Scatter plot of measured against modelled significant wave heights (left) and wave directions (right) for the south-eastern grid. Black dotted lines are references while solid lines are the linearly fitted lines for the various model source terms

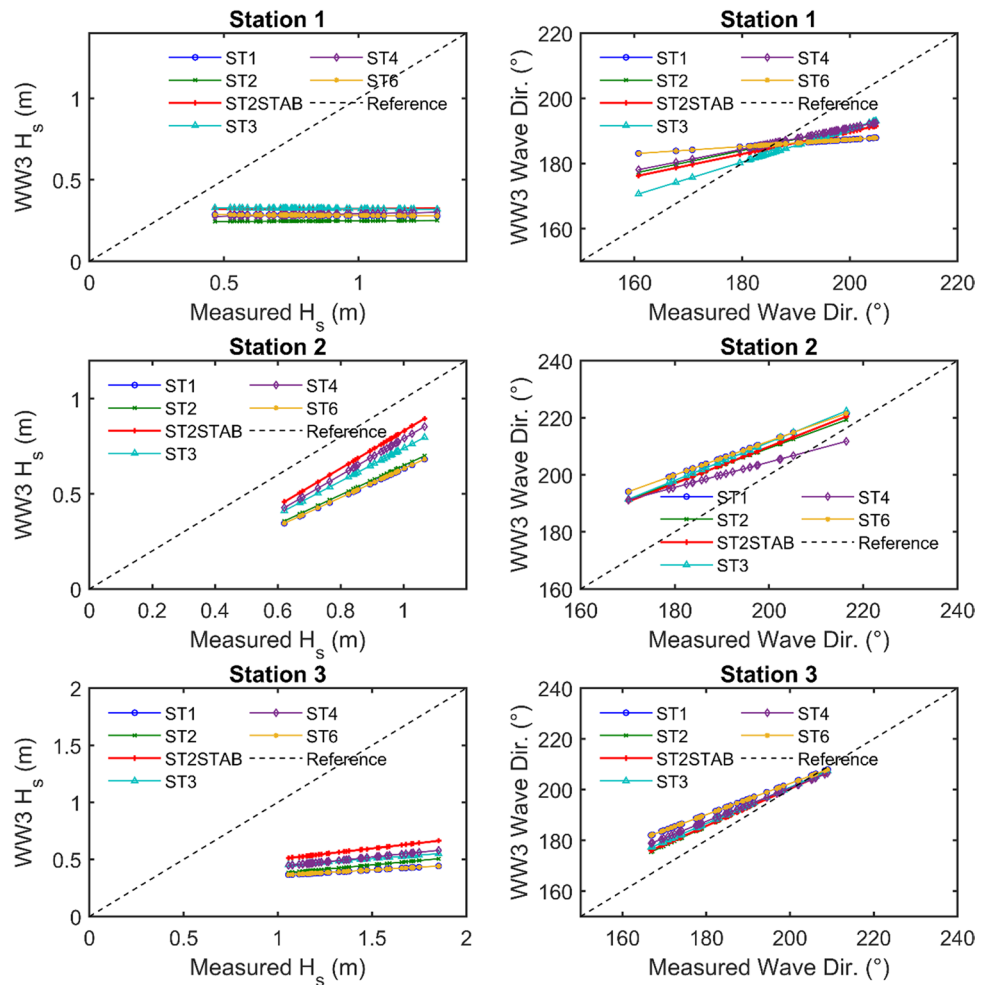
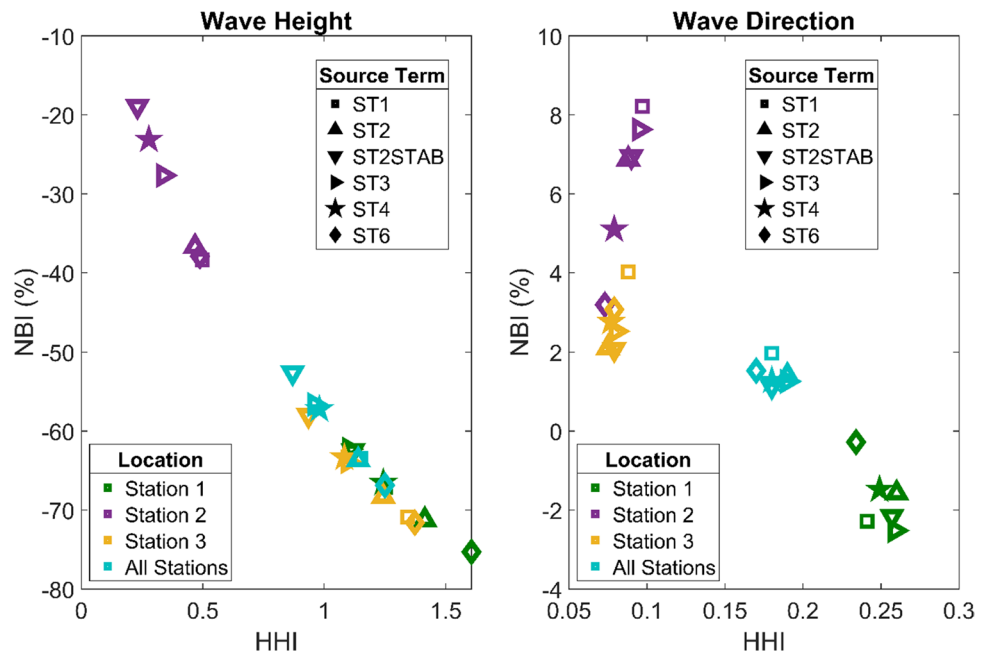


Fig. 15 Plots of HH against NBI for significant wave heights (left) and wave directions (right) for all stations of the south-eastern grid



spatial resolution (Tables 6 and 7). This is reflected in the mean bias, bias standard deviations and HH values at the respective stations. This may provide an evidence that the model generally performs better for larger spatial grids such as regional settings compared to smaller grids such as sub-regional or local settings with relatively finer output grid resolution. Or, on the other hand, it could indicate that wind interpolations on finer output grids may not necessarily translate into better performance of wave outputs. A similar situation was reported by Mentaschi et al. (2015) for the Mediterranean Sea where higher resolution interpolated wind fields did not necessarily result in improved “single point error indicator” such as the HH index for WW3 simulations. Indeed Holt and Cavaleri (1994) have indicated of this effect of wind interpolations on wave grid resolutions where coarser and finer resolutions in comparison with the original wind resolution smoothed out the peaks in wind distribution, resulting in underestimations of significant wave heights. This study and the findings of Mentaschi et al. (2015) could therefore suggest that the level of wind interpolation for sub-regional or local wave simulations may need to be considered and investigated for particular sub-regions/locations in order to determine the appropriate resolution required for the wave output when high-resolution wave outputs are to be generated from low-resolution wind forcing.

In general, ST2STAB has been observed as the input-dissipation source term that best estimates significant wave heights as well as wave direction for both the north-western and south-eastern sub-grids. For the entire West Africa grid however, while ST2STAB best estimates the significant wave heights, ST6 best estimates the wave directions.

The model run time required for the various input-dissipation source terms to fully execute was also recorded. Figure 18 indicates that the ST3 has the shortest model run time. This is followed closely by ST1 and ST2STAB, respectively, while ST4STAB has the longest. This is applicable to the entire West Africa grid as well as the two sub-grids. ST2STAB with its average run-time performance is therefore well placed to accurately estimate the wave heights and directions for the West Africa region in a relatively timely manner although it may not be the fastest.

4 Summary and Conclusions

This study investigates the input-dissipation source terms employed in the forecast and hindcast of ocean wave properties within the context of the West Africa region using the WAVEWATCH III numerical wave model. Seven variants of the input-dissipation source terms parameterized in WW3 were investigated in order to arrive at the source term(s) that best describe the nature of the ocean waves in the entire West Africa region as well as two sub-divisions of the region (north-western and south-eastern sections of the study area). Results of the simulations are compared graphically and statistically with in situ measurements taken at four different locations (stations) within the study area.

Comparisons of model outputs for all source terms with measurements show better agreements at station 4, located within the north-western section, compared to the other stations which are located within the south-eastern section. In the south-eastern section, station 2 also demonstrated better agreements, relative to stations 1 and 3. The differences in

Table 6 Summary of wave height statistics for comparisons of model simulations with in situ measurements for south-eastern and north-western sub-grids of West Africa grid

Model grid	Location	Source term	Mean bias (<i>m</i>)	Bias standard deviation (<i>m</i>)	Correlation coefficient (<i>r</i>)	HH index	NBI (%)
South-east	Station 1	ST1	−0.58	0.22	−0.02	1.253	−67.11
		ST2	−0.61	0.23	0.01	1.414	−71.23
		ST2STAB	−0.54	0.24	0.01	1.119	−62.48
		ST3	−0.54	0.23	−0.02	1.104	−62.3
		ST4	−0.57	0.24	0.04	1.243	−66.54
		ST6	−0.65	0.23	0.01	1.606	−75.31
	Station 2	ST1	−0.34	0.08	0.76*	0.497	−38.39
		ST2	−0.33	0.07	0.79*	0.468	−36.69
		ST2STAB	−0.17	0.08	0.81*	0.231	−18.91
		ST3	−0.25	0.08	0.79*	0.338	−27.67
		ST4	−0.21	0.08	0.82*	0.278	−23.13
		ST6	−0.34	0.08	0.81*	0.488	−37.89
	Station 3	ST1	−0.96	0.23	0.21	1.344	−70.88
		ST2	−0.92	0.24	0.24	1.243	−68.28
		ST2STAB	−0.78	0.26	0.23	0.935	−58.01
		ST3	−0.86	0.24	0.2	1.097	−63.88
		ST4	−0.86	0.25	0.22	1.083	−63.34
		ST6	−0.97	0.24	0.23	1.373	−71.6
	All south-east stations	ST1	−0.65	0.31	0.18	1.15	−63.47
		ST2	−0.65	0.3	0.29*	1.14	−63.65
		ST2STAB	−0.54	0.31	0.31*	0.87	−52.6
ST3		−0.58	0.31	0.24*	0.96	−56.64	
ST4		−0.59	0.32	0.26*	0.98	−57.23	
ST6		−0.69	0.31	0.24*	1.25	−66.87	
North-west	Station 4	ST1	−0.67	0.15	0.96*	0.405	−33.83
		ST2	−0.53	0.14	0.97*	0.305	−26.6
		ST2STAB	−0.12	0.23	0.97*	0.128	−6.1
		ST3	−0.36	0.19	0.97*	0.217	−18.37
		ST4	−0.24	0.15	0.97*	0.144	−11.95
		ST6	−0.4	0.16	0.97*	0.23	−20.09

*Indicates significant correlations, i.e. $p < 0.05$

the general performance of the model inputs at the various locations of the study area may be attributable to the accuracy of the wind input (Desbiolles et al., 2014; Tolman et al., 2002), the accuracy in the bathymetry (Arbic et al., 2019; Chen et al., 2018; Herterich & Dias, 2019) as well as other local factors such as ocean currents (Chen, 2018; Viitak et al., 2016; Zhang et al., 2021) that may largely influence wave model projections. The NCEP model winds used for simulating the wave model have been observed to perform better in the north-western section (Stn4) compared with the south-eastern section (Stn1, Stn2 and Stn3), thus being a major suspected contributor to the performance of the wave model outputs at these sub-divisions of the study area.

The ST3 source term is found to be computationally faster than all the other input-dissipation source terms. This is followed by ST1, with ST2STAB taking the third position. The slowest however is found to be ST4STAB.

It is found that different source terms best estimate the significant wave heights and directions at the different locations where in situ data was collected. Overall, the ST2STAB input-dissipation source term is found to best estimate the significant wave heights, whereas ST6 best estimates the wave directions of the entire West Africa region. These are therefore suitable for ocean wave modelling (forecasting and hindcasting) for the entire region. For the sub-grids, ST2STAB best estimate wave heights for both north-western and south-eastern sub-grids, whereas ST2STAB and ST6, respectively, best estimate wave directions for the north-western and south-eastern sub-grids.

It has been shown that the source term that best estimates the significant wave height at a location, especially for the West Africa region, may not necessarily be the best estimator of wave directions. However, the differences in the accuracy of wave direction estimations with the various

Table 7 Summary of wave direction statistics for comparisons of model simulations with in situ measurements for south-eastern and north-western sub-grids of West Africa grid

Model grid	Location	Source term	Mean bias (°)	Bias standard deviation (°)	Correlation coefficient (<i>r</i>)	HH index	NBI (%)
South-east	Station 1	ST1	−4.34	45.56	0.02	0.24	−2.28
		ST2	−2.99	49.5	0.06	0.26	−1.57
		ST2STAB	−4.11	48.75	0.07	0.26	−2.16
		ST3	−4.8	48.9	0.1	0.26	−2.52
		ST4	−2.81	47.49	0.06	0.25	−1.48
		ST6	−0.53	45.02	0.11	0.23	−0.28
	Station 2	ST1	15.65	11.33	0.52*	0.097	8.21
		ST2	13.11	11.58	0.52*	0.088	6.88
		ST2STAB	13.23	12.14	0.51*	0.09	6.94
		ST3	14.53	12.21	0.52*	0.095	7.63
		ST4	9.73	12.32	0.4*	0.079	5.1
		ST6	6.07	13.09	0.35	0.073	3.19
	Station 3	ST1	7.51	15.28	0.48*	0.088	4.02
		ST2	3.94	13.83	0.59*	0.075	2.11
		ST2STAB	3.86	14.61	0.55*	0.079	2.07
		ST3	4.71	14.59	0.54*	0.08	2.52
		ST4	5.16	13.79	0.54*	0.077	2.76
		ST6	5.74	14.03	0.55*	0.079	3.07
	All south-east stations	ST1	3.74	33.45	0.13	0.18	1.97
		ST2	2.67	35.38	0.18	0.19	1.41
		ST2STAB	2.15	35.14	0.18	0.18	1.13
		ST3	2.38	35.41	0.19*	0.19	1.26
		ST4	2.43	33.97	0.16	0.18	1.28
		ST6	2.9	32.23	0.19*	0.17	1.53
North-west	Station 4	ST1	−0.47	7.23	1*	0.172	−1.14
		ST2	0.32	6.48	1*	0.152	0.77
		ST2STAB	0.32	6.34	1*	0.149	0.77
		ST3	0.03	6.45	1*	0.152	0.06
		ST4	−0.03	6.61	1*	0.156	−0.08
		ST6	−0.19	7.16	1*	0.169	−0.47

*Indicates significant correlations, i.e. $p < 0.05$

input-dissipation source terms have been observed to be very minimal compared to those of wave height estimations, and therefore the best source term that estimates wave heights can equally be used in estimating the wave directions without any significant impact in accuracies.

Although statistically ST2STAB and ST6 have been identified as the input-dissipation source terms that best estimate the significant wave heights and the wave directions respectively for the entire West Africa grid, it would be prudent to use ST2STAB as the main source term for estimating both the significant wave heights and wave directions. This is also because ST2STAB follows ST6 very closely in estimating wave directions for the combined locations of the south-eastern grid. Moreover, little variations exist among all the input-dissipation source terms in estimating wave directions for the region as compared to those of wave height estimations. In effect,

ST2STAB is capable of accurately estimating the wave heights and directions with respect to the larger West Africa grid. It should however be noted that this is mainly applicable at the regional level. Although ST2STAB has been identified to best estimate the wave parameters of the entire West Africa region, it is recommended that further investigations be conducted into the wind speed correction parameter of this source term for proper calibration as indicated by Wang et al. (2017), to fit the region. This would lead to an improvement in the wave model outputs.

As has been demonstrated by this study, the input-dissipation terms will vary at different locations on local or sub-regional levels of the West Africa region, and thus ocean wave model outputs will perform better if the right source term is investigated and used rather than relying on global input-dissipation parameterizations or global datasets for sub-regional or local-scale investigations or applications.

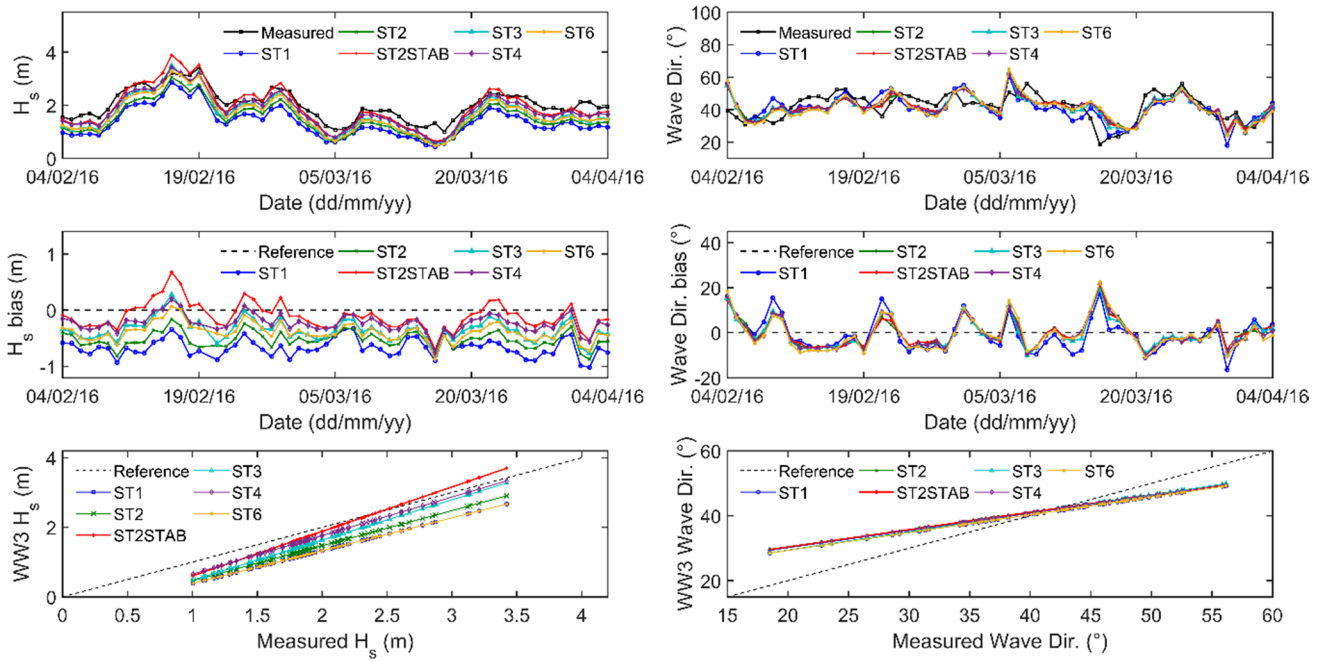
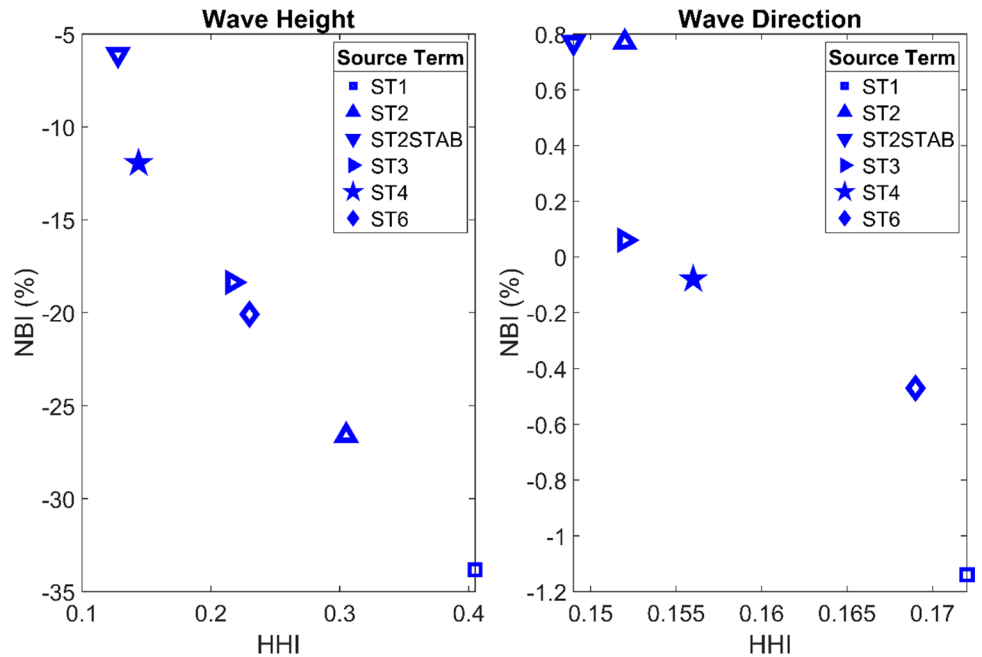


Fig. 16 Plots of significant wave heights (left) and wave directions (right) for the north-western grid. Top: Time-series of significant wave heights and directions; Middle: Time-series of residuals of sig-

nificant wave heights and directions; Bottom: Scatter plots of measured against modelled significant wave heights and directions

Fig. 17 Plots of HH against NBI for significant wave heights (left) and wave directions (right) for the north-western grid

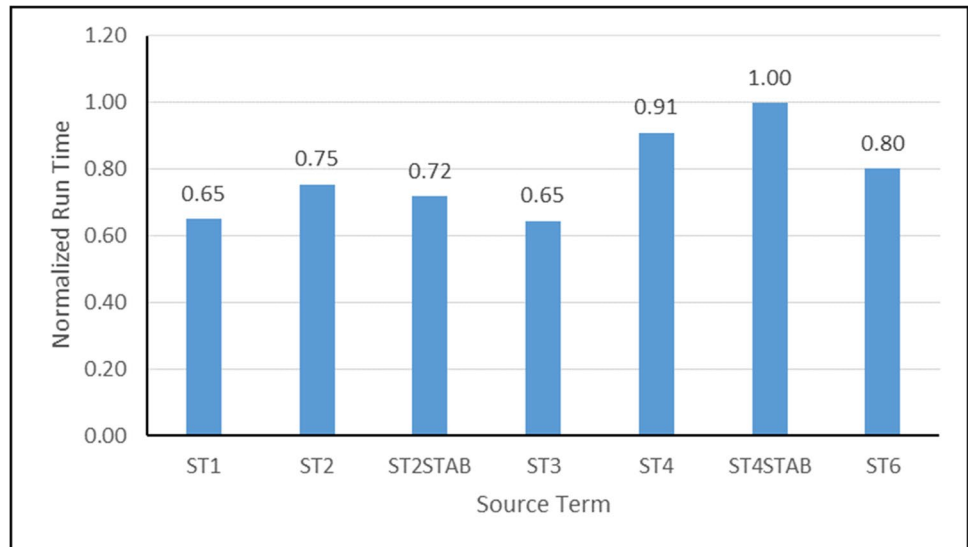


It is observed that the input-dissipation source terms have higher degrees of underestimation of significant wave heights compared to lower degrees of underestimation and overestimation of wave directions. This implies that the model parameterizations generally predict wave directions more accurately than it does for the wave heights for the

study area. This is however only in respect of the input-dissipation source term investigations.

The model outputs in this study are observed to generally perform better on relatively larger spatial grids compared to relatively smaller finer grids. This was noted

Fig. 18 Summary of overall model run-time performance of input-dissipation source terms investigated. Run time is normalized by the maximum time of 136,113.05 s



when simulation outputs of sub-grids were compared with those of the entire West Africa grid using the same model parameterization schemes. With this assertion supported by the findings of Mentaschi et al. (2015), it may be necessary to investigate the appropriate level of wind interpolation to determine the final grid resolution of the wave outputs on sub-regional levels.

Acknowledgements We thank the Department of Marine and Fisheries Sciences of the University of Ghana, as well as the Regional Marine Centre at the University of Ghana for making buoy data from Ghana and Cabo Verde available. Thanks also to the International Marine and Dredging Consultants (IMDC) for making available ADCP data from Ghana. Thanks to Dr. Zacharie Sohou of IRHOB, Benin, for making buoy data from Benin available under the auspices of the GMES and Africa programme.

The wave model run computations was done using high-performance computing (HPC) resources provided by the University of Ghana and the West African Centre for Cell Biology of Infectious Pathogens (WACCBIP) programme. Additional cloud computing and HPC resources was provided by the EU sponsored WEkEO Copernicus DIAS and the Center for High Performance Computing (CHPC) in South Africa through the Weather, Climate and Water (ERTH0955) group of CHPC.

Thanks also to Prof. Benjamin L. Lamptey of the School of Earth and Environment, University of Leeds, and formerly of the Ghana Meteorological Agency and Regional Maritime University both in Ghana, and the African Centre of Meteorological Applications for Development (ACMAD) in Niamey, Niger, for facilitating access to the CHPC.

The study was supported by the Global Monitoring for Environment and Security and Africa (GMES & Africa) programme at the University of Ghana. Partial financial support was provided by the Open Society Foundation (OSF) under the Enhancing Efficiency and Effectiveness—Climate Change and Sustainability Development (EEE-CCSD) project. This study is part of the PhD. thesis of Bennet Atsu Kwame Foli.

We also thank the anonymous reviewers whose comments helped improve the manuscript.

Availability of Data and Material In this paper, wind data used for model simulation were downloaded from the National Oceanic and Atmospheric Administration (NOAA) National Operational Model Archive and Distribution System (NOMADS) server, https://polar.ncep.noaa.gov/waves/hindcasts/multi_1/; Satellite observed wave data were obtained from the Archiving, Validation and Interpretation of Satellite Oceanographic data (AVISO) web portal, <https://www.aviso.altimetry.fr/es/data/products/wind/wave-products/mswh/mwind.html>; Satellite observed wind data were obtained from IFREMER web portal, <ftp://ftp.ifremer.fr/ifremer/cersat/products/gridded/MWF/L3/ASCAT/Daily/Netcdf/>; and PIRATA meteorological buoy data were obtained from https://ftp1.ifremer.fr/Core/INSITU_GLO_NRT_OBSERVATIO_NS_013_030/history/mooring/. The datasets generated and analysed during the current study are available from the corresponding author on reasonable request. Data analysis and figures were generated using MATLAB®.

Declarations

Conflict of Interest The authors declare no competing interests.

References

- Arbic BK, Fringer OB, Klymak JM, Mayer FT, Trossman DS, Zhu P (2019) Connecting process models of topographic wave drag to global eddying general circulation models. *Oceanography* 32(4):145–155
- Arduin, F., Rogers, E., Babanin, A. V., Filipot, J.-F. F., Magne, R., Roland, A. A. A., Van Der Westhuysen, A., Queffeuou, P., Lefevre, J.-M. M., Aouf, L., & Collard, F. (2010). Semiempirical dissipation source functions for ocean waves. Part I: Definition, calibration, and validation. *Journal of Physical Oceanography*, 40(9), 1917–1941. <https://doi.org/10.1175/2010JPO4324.1>
- Battjes, J. A., & Janssen, J. P. F. M. (1978). Energy loss and set-up due to breaking of random waves. *Proc. 16th Int. Conf. Coastal Eng.*, 569–587.
- Bidlot, J.-R., Janssen, P., & Abdalla, S. (2007). *A revised formulation of ocean wave dissipation and Its Model Impact* (Issue January).

- Cardone H, Graber C, Jensen RE, Hasselmann S, Caruso MJ (1995) In search of the true surface wind field in SWADE IOP-1: ocean wave modelling perspective. *Global Ocean Atmos. Syst.* 3:107–150
- Cavaleri, L., & Malanotte-Rizzoli, P. (1981). Wind wave prediction in shallow water: theory and application. *Journal of Geophysical Research*, 86(C11)(C11), 10961–10973.
- Cavaleri Luigi, Bertotti L, Lionello P (1991) Wind wave cast in the Mediterranean Sea. *Journal of Geophysical Research* 96(C6):10739–10764. <https://doi.org/10.1029/91jc00322>
- Chalikov DV (1995) The parameterization of the wave boundary layer. *Journal of Physical Oceanography* 25:1333–1349
- Chalikov DV, Belevich MY (1993) One-dimensional theory of the wave boundary layer. *Bound. Layer Meteor.* 63:65–96
- Chawla A, Tolman H (2007) Automated grid generation for WAVEWATCH III. *NWS Tech. Note* 254:1–77
- Chen C (2018) Case study on wave-current interaction and its effects on ship navigation. *Journal of Hydrodynamics* 30(3):411–419. <https://doi.org/10.1007/s42241-018-0050-5>
- Chen JL, Ralston DK, Geyer WR, Sommerfield CK, Chant RJ (2018) Wave generation, dissipation, and disequilibrium in an embayment with complex bathymetry. *Journal of Geophysical Research: Oceans* 123:7856–7876. <https://doi.org/10.1029/2018JC014381>
- Desbiolles F, Blanke B, Bentamy A (2014) Short-term upwelling events at the western African coast related to synoptic atmospheric structures as derived from satellite observations. *Journal of Geophysical Research: Oceans* 119(1):461–483. <https://doi.org/10.1002/2013JC009278>
- Foli BAK, Appeaning Addo K, Ansong JK, Wiawe G (2021) Evaluation of ECMWF and NCEP reanalysis wind fields for long-term historical analysis and ocean wave modelling in West Africa. *Remote Sensing in Earth Systems Sciences*. <https://doi.org/10.1007/s41976-021-00052-3>
- Günther, H., Hasselmann, S., & Janssen, P. A. E. M. (1992). *The WAM model cycle 4*. https://inis.iaea.org/search/search.aspx?orig_q=RN:26000788
- Hanna, S. R., & Heinold, D. W. (1985). *Development and application of a simple method for evaluating air quality models* (4409th ed.). American Petroleum Institute.
- Hasselmann K, Barnett TP, Bouws E, Carlson H, Cartwright DE, Enke K, Ewing JA, Gienapp H, Hasselmann DE, Kruseman P, Meerburg A, Muller P, Olbers DJ, Richter K, Sell W, Walden H (1973) Measurement of wind-wave growth and swell decay during the Joint North Sea Wave Project (JONSWAP). *Deutsches Hydrographisches Institut* 12:399–404. <https://doi.org/10.1016/j.coastaleng.2016.06.001>
- Hasselmann S, Hasselmann K, Allender JH, Barnett TP (1985) Computations and parameterizations of the nonlinear energy transfer in a gravity-wave spectrum. Part II: parameterizations of the nonlinear energy transfer for application in wave models. *J Phys Oceanogr* 15(11):1378–1391. [https://doi.org/10.1175/1520-0485\(1985\)015<1378:CAPOTN>2.0.CO;2](https://doi.org/10.1175/1520-0485(1985)015<1378:CAPOTN>2.0.CO;2)
- Herterich JG, Dias F (2019) Extreme long waves over a varying bathymetry. *Journal of Fluid Mechanics* 878:481–501. <https://doi.org/10.1017/jfm.2019.618>
- Holt, M., & Cavaleri, L. (1994). Wind interpolation. In G. Komen, L. Cavaleri, M. Donelan, K. Hasselmann, S. Hasselmann, & P. Janssen (Eds.), *Dynamics and modelling of ocean waves* (pp. 299–300). Cambridge University Press. <https://doi.org/10.1017/CBO9780511628955>
- Janssen PAEM (1989) Wave-induced stress and the drag of air flow over sea waves. *Journal of Physical Oceanography* 19(6):745–772
- Janssen PAEM (1991) Quasi-linear theory of wind-wave generation applied to wave forecasting. *J Phys Oceanogr* 21(11):1631–1642. [https://doi.org/10.1175/1520-0485\(1991\)021<1631:QLTOWW>2.0.CO;2](https://doi.org/10.1175/1520-0485(1991)021<1631:QLTOWW>2.0.CO;2)
- Kalourazi MY, Siadatmousavi SM, Yeganeh-Bakhtiary A, Jose F (2020) WAVEWATCH-III source terms evaluation for optimizing hurricane wave modeling: a case study of Hurricane Ivan. *Oceanologia*, In press. <https://doi.org/10.1016/j.oceano.2020.12.001>
- Komem GK, Hasselmann S, Hasselmann K (1984) On the existence of a fully developed wind-sea spectrum. *Journal of Physical Oceanography* 14:1271–1285
- Kuznetsova A, Baydakov G, Papko V, Kandaurov A, Vdovin M, Sergeev D, Troitskaya Y (2016) Adjusting of wind input source term in WAVEWATCH III model for the middle-sized water body on the basis of the field experiment. *Advances in Meteorology* 2016. <https://doi.org/10.1155/2016/8539127>
- Lee HS (2015) Evaluation of WAVEWATCH III performance with wind input and dissipation source terms using wave buoy measurements for October 2006 along the East Korean coast in the East Sea. *Ocean Engineering* 100:67–82. <https://doi.org/10.1016/j.oceaneng.2015.03.009>
- Liu Q, Babanin A, Fan Y, Zieger S, Guan C, Moon IJ (2017) Numerical simulations of ocean surface waves under hurricane conditions: assessment of existing model performance. *Ocean Modelling* 118:73–93. <https://doi.org/10.1016/j.ocemod.2017.08.005>
- Liu Q, Rogers WE, Babanin AV, Young IR, Romero L, Zieger S, Qiao F, Guan C (2019) Observation-based source terms in the third-generation wave model WAVEWATCH III: updates and verification. *Journal of Physical Oceanography* 49(2):489–517. <https://doi.org/10.1175/JPO-D-18-0137.1>
- Longuet-Higgins MS, Stewart RW (1961) The changes in amplitude of short gravity waves on steady non-uniform currents. *J. Fluid Mech.* 10(4):529–549
- Longuet-Higgins MS, Stewart RW (1962) Radiation stress and mass transport in gravity waves, with application to 'surf-beats'. *J. Fluid Mech.* 13(4):481–504
- Mentaschi L, Besio G, Cassola F, Mazzino A (2013) Problems in RMSE-based wave model validations. *Ocean Modelling* 72:53–58. <https://doi.org/10.1016/j.ocemod.2013.08.003>
- Mentaschi Lorenzo, Besio G, Cassola F, Mazzino A (2015) Performance evaluation of Wavewatch III in the Mediterranean Sea. *Ocean Modelling* 90:82–94. <https://doi.org/10.1016/j.ocemod.2015.04.003>
- Montoya RD, Arias AO, Royero JCO, Ocampo-Torres FJ (2013) A wave parameters and directional spectrum analysis for extreme winds. *Ocean Engineering* 67:100–118. <https://doi.org/10.1016/j.oceaneng.2013.04.016>
- National Weather Service. (2009). *WAVEWATCH III® Model*. <https://polar.ncep.noaa.gov/waves/wavewatch/>
- Olagnon, M., Prevosto, M., Van-Iseghem, S., Ewans, K., & Forristall, G. Z. (2004). *WASP -West Africa Swell Project – Final report and Appendices*. <http://archimer.ifremer.fr/doc/00114/22537/>
- Ondoa, G. A., Bonou, F., Tomety, F. S., du Penhoat, Y., Perret, C., Degbe, C. G. E., & Almar, R. (2017). Beach response to wave forcing from event to inter-annual time scales at Grand Popo, Benin (Gulf of Guinea). *Water (Switzerland)*, 9(6). <https://doi.org/10.3390/w9060447>
- Ponce de León S, Guedes Soares C, Soares CG (2008) Sensitivity of wave model predictions to wind fields in the Western Mediterranean sea. *Coastal Engineering* 55(11):920–929. <https://doi.org/10.1016/j.coastaleng.2008.02.023>
- Rutledge GK, Alpert J, Ebisuzaki W (2006) NOMADS: a climate and weather model archive at the National Oceanic and Atmospheric Administration. *Bulletin of the American Meteorological Society* 87(3):327–341. <https://doi.org/10.1175/BAMS-87-3-327>
- Schmidt KM, Swart S, Reason C, Nicholson S-AA (2017) Evaluation of satellite and reanalysis wind products with in situ wave glider wind observations in the southern ocean. *Journal of Atmospheric*

- and Oceanic Technology 34(12):2551–2568. <https://doi.org/10.1175/JTECH-D-17-0079.1>
- Semedo A (2018) Seasonal variability of wind sea and swell waves climate along the canary current: the local wind effect. *Journal of Marine Science and Engineering* 6(1):28. <https://doi.org/10.3390/jmse6010028>
- Sheng Y, Shao W, Li S, Zhang Y, Yang H, Zuo J (2019) Evaluation of typhoon waves simulated by WaveWatch-III Model in shallow waters around Zhoushan Islands. *Journal of Ocean University of China* 18(2):365–375. <https://doi.org/10.1007/s11802-019-3829-2>
- Snyder, R. L., Dobson, F. W., Elliott, J. A., & Long, R. B. (1981). Array measurements of atmospheric pressure fluctuations above surface gravity waves. *Journal of Fluid Mechanics*, 102, 1–59. 0022-1120/81/4577-2590
- Stopa JE, Ardhuin F, Babanin A, Zieger S (2016) Comparison and validation of physical wave parameterizations in spectral wave models. *Ocean Modelling* 103:2–17. <https://doi.org/10.1016/j.ocemod.2015.09.003>
- Swain J, Umesh PA, J, S., & PA, U. (2018) Prediction of uncertainty using the third generation wave model WAVEWATCH III driven by ERA-40 and blended winds in the North Indian Ocean. *Journal of Oceanography and Marine Research* 06(01):1–17. <https://doi.org/10.4172/2572-3103.1000173>
- Tolman HL (2002) Alleviating the garden sprinkler effect in wind wave models. *Ocean Modelling* 4(3–4):269–289. [https://doi.org/10.1016/S1463-5003\(02\)00004-5](https://doi.org/10.1016/S1463-5003(02)00004-5)
- Tolman HL, Balasubramanian B, Burroughs LD, Chalikov DV, Chao YY, Chen HS, Gerald VM (2002) Development and implementation of wind-generated ocean surface wave models at NCEP. *Weather and Forecasting* 17(2):311–333. [https://doi.org/10.1175/1520-0434\(2002\)017%3c0311:daiowg%3e2.0.co;2](https://doi.org/10.1175/1520-0434(2002)017%3c0311:daiowg%3e2.0.co;2)
- Tolman HL, Chalikov D (1996) Source terms in a third-generation wind wave model. *J Phys Oceanogr* 26(11):2497–2518. [https://doi.org/10.1175/1520-0485\(1996\)026<2497:STIATG>2.0.CO;2](https://doi.org/10.1175/1520-0485(1996)026<2497:STIATG>2.0.CO;2)
- Toualy E, Aman A, Koffi P, Marin F, Wango TE (2015) Ocean swell variability along the northern coast of the Gulf of Guinea. *African Journal of Marine Science* 37(3):353–361. <https://doi.org/10.2989/1814232X.2015.1074940>
- Umesh PA, Behera MR (2020) Performance evaluation of input-dissipation parameterizations in WAVEWATCH III and comparison of wave hindcast with nested WAVEWATCH III-SWAN in the Indian Seas. *Ocean Engineering* 202:1–29. <https://doi.org/10.1016/j.oceaneng.2020.106959>
- Umesh PA, Swain J, Balchand AN (2018) Inter-comparison of WAM and WAVEWATCH-III in the North Indian Ocean using ERA-40 and QuikSCAT/NCEP blended winds. *Ocean Engineering* 164(June):298–321. <https://doi.org/10.1016/j.oceaneng.2018.06.053>
- Viitak, M., Maljutenko, I., Alari, V., Suursaar, Ü., Rikka, S., & Lagemaa, P. (2016). The impact of surface currents and sea level on the wave field evolution during St. Jude storm in the eastern Baltic Sea. *Oceanologia*, 58(3), 176–186. <https://doi.org/10.1016/j.oceano.2016.01.004>
- Wang J, Zhang J, Yang J, Bao W, Wu G, Ren Q (2017) An evaluation of input/dissipation terms in WAVEWATCH III using in situ and satellite significant wave height data in the South China Sea. *Acta Oceanologica Sinica* 36(3):20–25. <https://doi.org/10.1007/s13131-017-1038-7>
- WAVEWATCH III Development Group. (2016). *User manual and system documentation of WAVEWATCH III version 5.16* (Tech. Note). NOAA/NWS/NCEP/MMAB.
- Zhang H, He H, Zhang WZ, Tian D (2021) Upper ocean response to tropical cyclones: a review. *Geoscience Letters* 8(1):1–12. <https://doi.org/10.1186/s40562-020-00170-8>
- Zieger, S., Babanin, A. V., Erick Rogers, W., & Young, I. R. (2015). Observation-based source terms in the third-generation wave model WAVEWATCH. *Ocean Modelling*, 96(July 2015), 2–25. <https://doi.org/10.1016/j.ocemod.2015.07.014>

Publisher's Note Springer Nature remains neutral with regard to jurisdictional claims in published maps and institutional affiliations.